Comparative Transcriptomics Analyses across Species, Organs, and Developmental Stages Reveal Functionally Constrained lncRNAs

Fabrice Darbellay, Anamaria Necsulea

Article

Comparative transcriptomics analyses across species, organs and developmental stages reveal functionally constrained lncRNAs

Fabrice Darbellay[1,$,*] and Anamaria Necsulea[1,2,*]

[1]School of Life Sciences, École Polytechnique Fédérale de Lausanne (EPFL), Lausanne, Switzerland

[2]Université de Lyon, Université Lyon 1, CNRS, Laboratoire de Biométrie et Biologie Évolutive UMR 5558, F-69622 Villeurbanne, France

[$]Present address: Environmental Genomics and Systems Biology Division, Lawrence Berkeley National Laboratory, 1 Cyclotron Road, Berkeley, California 94720, USA.

[*]Corresponding authors:
Fabrice Darbellay (fdarbellay@lbl.gov)
Anamaria Necsulea (anamaria.necsulea@univ-lyon1.fr)

Running title: Functionally constrained lncRNAs in embryonic development

Keywords: long non-coding RNAs; evolution; development; comparative transcriptomics.

Abstract

The functionality of long non-coding RNAs (lncRNAs) is disputed. In general, lncRNAs are under weak selective pressures, suggesting that the majority of lncRNAs may be non-functional. However, although some surveys showed negligible phenotypic effects upon lncRNA perturbation, key biological roles were demonstrated for individual lncRNAs. Most lncRNAs with proven functions were implicated in gene expression regulation, in pathways related to cellular pluripotency, differentiation and organ morphogenesis, suggesting that functional lncRNAs may be more abundant in embryonic development, rather than in adult organs. To test this hypothesis, we perform a multi-dimensional comparative transcriptomics analysis, across five developmental time-points (two embryonic stages, newborn, adult and aged individuals), four organs (brain, kidney, liver and testes) and three species (mouse, rat and chicken). We find that, overwhelmingly, lncRNAs are preferentially expressed in adult and aged testes, consistent with the presence of permissive transcription during spermatogenesis. LncRNAs are often differentially expressed among developmental stages and are less abundant in embryos and newborns compared to adult individuals, in agreement with a requirement for tighter expression control and less tolerance for noisy transcription early in development. For differentially expressed lncRNAs, we find that the patterns of expression variation among developmental stages are generally conserved between mouse and rat. Moreover, lncRNAs expressed above noise levels in somatic organs and during development show higher evolutionary conservation, in particular at their promoter regions. Thus, we show that functionally constrained lncRNA loci are enriched in developing organs, and we suggest that many of these loci may function in an RNA-independent manner.

Introduction

Long non-coding RNAs (lncRNAs, loosely defined as transcripts without protein-coding potential, at least 200 nucleotides long) are an excellent illustration of the ongoing conceptual tug-of-war between biochemical activity and biological function (Graur et al. 2013; Doolittle 2018). Recent sequencing-based studies identified thousands of lncRNAs in vertebrates (Guttman et al. 2009; Khalil et al. 2009; Iyer et al. 2015; Pertea et al. 2018). While this class of transcripts includes lncRNAs with undisputed biological roles, such as *Xist* (Brown et al. 1991) or *H19* (Brannan et al. 1990), experimental validations are lacking for the great majority of lncRNAs and their functionality is controversial.

The first functional characterizations of individual lncRNAs forged the idea that they are important contributors to gene expression regulatory networks. This has been unequivocally proven for some lncRNAs, such as *Xist*, whose transcription and subsequent coating of the X chromosome triggers a complex chain of molecular events leading to X inactivation in placental mammals (Munschauer et al. 2018). Other proposed mechanisms for gene expression regulation by lncRNAs include directing chromatin-modifying complexes at specific genomic locations, to control gene

expression in *trans* (Rinn et al. 2007); providing decoy targets for microRNAs (Cesana et al. 2011); enhancing neighboring gene expression through an RNA-dependent mechanism (Ørom et al. 2010). Biological functions unrelated to gene expression regulation were also proposed for lncRNAs. For example, the NORAD lncRNA was shown to assemble a topoisomerase complex critical for genome stability (Munschauer et al. 2018), while the X-linked Firre lncRNA is involved in chromatin super-loop formation on the inactive X chromosome (Hacisuleyman et al. 2014; Barutcu et al. 2018). Additional evidence that individual lncRNAs are undoubtedly biologically relevant comes from associations with human diseases, including cancer, as for the SAMMSON lncRNA (Vendramin et al. 2018).

Initial studies of lncRNA functionality generally asserted that biological functions are directly carried out by the transcribed RNA molecules. For some lncRNAs, this hypothesis was supported by thorough functional tests, including rescue experiments showing that phenotypic effects of lncRNA locus deletion can be reversed by expressing the lncRNAs *in trans* (Munschauer et al. 2018). Thus, for a subset of lncRNA loci, their biological function is undoubtedly achieved by the non-coding RNA molecule. However, in some cases, lncRNA function resides in the act of transcription at a given genomic location, rather than in the product of transcription (Latos et al. 2012). In other cases, biological functions are carried out by other elements embedded in the lncRNA genomic loci (Bassett et al. 2014). For example, transcription of *Linc-p21*, originally described as a *cis*-acting enhancer lncRNA, is not needed to regulate neighboring gene expression, which is instead controlled by multiple enhancer elements within the locus (Groff et al. 2016). Genetic engineering of multiple lncRNA loci in mouse likewise indicated that lncRNA transcripts are dispensable, and that gene expression regulation by lncRNA loci is instead achieved by the process of transcription and splicing, or by additional regulatory elements found in lncRNA promoters (Engreitz et al. 2016; Anderson et al. 2016). Furthermore, some attempts to look for lncRNA function through genetic engineering approaches showed that the tested lncRNA loci are altogether dispensable (Amândio et al. 2016; Zakany et al. 2017; Goudarzi et al. 2019). These recent observations signal a paradigm shift in lncRNA biology, as it is increasingly acknowledged that, even when phenotypic effects can be unambiguously mapped to lncRNA loci, they may not be driven by the lncRNA transcripts themselves.

Importantly, this new perspective on lncRNA biology had been predicted by evolutionary analyses, traditionally used to evaluate the functionality of diverse genomic elements (Haerty and Ponting 2014; Ulitsky 2016). Evolutionary studies of lncRNAs in vertebrates agree that selective constraint on lncRNA primary sequences is weak, though significantly above the genomic background (Ponjavic et al. 2007; Kutter et al. 2012; Necsulea et al. 2014; Washietl et al. 2014; Hezroni et al. 2015). These observations are compatible with the hypothesis that many of the lncRNAs detected with sensitive transcriptomics techniques may be non-functional noise (Ponjavic et al. 2007), or that their function is carried out by small conserved elements, such that the selective constraint signal on the

entire lncRNA locus is overall weak (Ulitsky 2016). They also indicate that lncRNA functionality may not reside in the primary transcribed sequence. Indeed, mammalian lncRNA promoters show higher levels of sequence conservation, similar to protein-coding gene promoters (Necsulea et al. 2014), as expected if they carry out additional regulatory functions independently of the transcribed RNA molecule. Moreover, it was previously reported that, in multi-exonic lncRNAs, splicing regulatory elements are more conserved than exonic sequences (Schüler et al. 2014; Haerty and Ponting 2015), in agreement with the recent finding that lncRNA splicing can contribute to neighboring gene regulation (Engreitz et al. 2016). Thus, detailed evolutionary analyses of lncRNA loci can bring insights into their functionality, and can help prioritize candidates for experimental validation.

Most comparative lncRNA studies were so far restricted to adult organ transcriptomes. These comparisons showed that lncRNAs are preferentially expressed in adult testes, during spermatogenesis (Soumillon et al. 2013). This process is characterized by a permissive chromatin environment, which can promote non-functional transcription (Soumillon et al. 2013). The resulting lncRNA datasets may thus be enriched in non-functional transcripts. Additional lines of evidence suggest that the search for functional lncRNAs should be extended beyond adult organ transcriptomes. For example, involvement in developmental phenotypes was proposed for many experimentally-tested lncRNAs (Sauvageau et al. 2013; Ulitsky et al. 2011; Grote et al. 2013), and an enrichment for developmental transcription factor binding was reported for the promoters of conserved lncRNAs (Necsulea et al. 2014). These observations motivated us to add a temporal dimension to comparative lncRNA transcriptomics studies. Therefore, here we characterize lncRNAs across species, organs and developmental stages. We analyze the spatial and temporal expression patterns of protein-coding genes and lncRNAs, in conjunction with their evolutionary conservation. We find that, while lncRNAs are overall poorly conserved during evolution in terms of primary sequence or expression patterns, higher frequencies of constrained lncRNAs are observed in embryonic transcriptomes. For many of these loci, biological function may be RNA-independent, as the highest levels of sequence conservation are observed on promoter regions and on splice signals, rather than on lncRNA exonic sequence. Our results are thus compatible with unconventional, RNA-independent functions for evolutionarily conserved lncRNA loci, in particular for those that are expressed during embryonic development.

Results

Comparative transcriptomics across species, organs and developmental stages

To study protein-coding and lncRNA expression patterns across both developmental and evolutionary time, we generated strand-specific RNA-seq data for mouse and rat, for four major organs (brain, kidney, liver and testes) and five developmental time points, including two embryonic stages, newborn, young and aged adult individuals (Figure 1A, Supplementary Table 1, Materials and

methods). The selected time points allow us to obtain a broad view of major organ ontogenesis and to capture drastic physiological changes during development (Theiler 1989). We chose to include in our study both young adult (8-10 weeks old) and aged adult individuals (12 to 24 months old), thus completing our overview of temporal patterns of gene expression variation. At the earliest embryonic stage (day 13.5 post-conception for mouse, day 15 for rat), we dissected only the three somatic organs. Our experimental design for mouse and rat thus comprises 19 organ / developmental stage combinations. To obtain a broader evolutionary perspective we generated comparable RNA-seq data for the chicken, for the two earliest developmental stages (Figure 1A, Supplementary Table 1). We generated between 2 and 4 biological replicates for each species/organ/developmental stage combination (Supplementary Table 1). Additional RNA-seq samples from previous publications were included in the lncRNA annotation process, to increase detection sensitivity (Supplementary Table 2).

The organs and developmental stages included in our study differ greatly in terms of their cellular composition diversity. To verify that our whole-organ RNA-seq data reflects cellular composition heterogeneity, we assessed the expression patterns of cell population markers derived from single-cell transcriptomics studies (Tabula Muris Consortium 2018; Green et al. 2018) in our samples (Supplementary Figure 1, Supplementary Table 3, Supplementary Methods). This analysis confirms that our transcriptome collection reflects expected developmental patterns. For example, mature oligodendrocyte cell markers are systematically highly expressed in adult brain, while oligodendrocyte precursor markers are more highly expressed in the earliest developmental stages (Supplementary Figure 1). To further characterize our transcriptome collection, we sought to identify genes that could serve as markers for organ/developmental stage combinations. To do this, we selected genes that have narrow expression distributions, and for which maximum expression is observed in the same organ/developmental stage combination in mouse and rat (Supplementary Methods, Supplementary Table 4). Gene ontology enrichment analyses for these lists of genes are coherent with the cellular composition and biological processes at work. Thus, genes involved in forebrain neuron differentiation are over-represented in the mid-stage embryonic brain, while processes related to synaptic transmission are enriched among genes specifically expressed in adult brain (Supplementary Figure 2). In the kidney, the early developmental stages are enriched in genes involved in metanephric development (Supplementary Figure 3). The newborn liver stands out due to its strong enrichment in genes involved in immune response, while metabolic processes are over-represented in the adult liver (Supplementary Figure 4). Embryonic testes samples express genes implicated in gamete generation and gene silencing by miRNAs, including the *Piwi*-like genes, while adult testes transcriptomes are dominated by genes involved in spermatogenesis (Supplementary Figure 5). These patterns confirm that our whole-organ transcriptome collection captures the cell composition changes and physiological transitions that occur during organ development.

Developmental expression patterns are well conserved among species for protein-coding genes

To gain a first glimpse into the evolution of developmental gene expression patterns, we performed a principal component analysis (PCA) for 10,363 protein-coding genes shared among mouse, rat and chicken (Figure 1B, Supplementary Methods). This analysis revealed that the main source of gene expression variability among species, organs and developmental stages is the distinction between adult and aged testes and the other samples, which are separated on the first PCA axis (Figure 1B). In contrast, embryonic and newborn testes are grouped with kidney samples from similar developmental stages, in agreement with the common developmental origin of the kidney and the gonads (Nel-Themaat et al. 2010). The first axis of the PCA, which explains 67% of the total expression variance, also correlates with the developmental stage for the brain: samples derived from adult and aged individuals have higher coordinates on this axis than embryonic and newborn samples (Figure 1B, Supplementary Figure 6, Kruskal-Wallis test p-value 0.003). The second PCA axis (10% explained variability) mainly reflects the difference between brain and the other organs, but is also associated with the developmental stage for kidney and liver (Figure 1B, Supplementary Figure 6, Kruskal-Wallis test p-value $4e^{-4}$ for kidney, $4e^{-5}$ for liver). However, we note that the association between PC2 and developmental stages for kidney and liver may be confounded by differences in RNA among developmental stages for these organs (Supplementary Methods, Supplementary Figure 6).

While mouse and rat samples are almost undistinguishable on the PCA factorial map, there is considerably higher expression divergence between chicken and the two rodent species (Figure 1B). However, differences among major organs are stronger than differences among species, even at these broad evolutionary distances: brain samples all cluster together, irrespective of the species of origin, and are clearly separated from kidney and liver samples on the second PCA axis (Figure 1B). These patterns of gene expression variations are confirmed by a hierarchical clustering analysis based on Spearman's correlation coefficients between pairs of samples (Figure 1C). The strongest clustering is observed for adult and aged testes samples, followed by brain samples (Figure 1C).

The grouping among samples derived from similar organs and developmental stages, irrespective of the species of origin, is stronger for genes that are associated with embryonic development and with gene expression regulation (Supplementary Methods, Supplementary Figure 6C, D). For this set of genes, both the principal component analysis and the hierarchical clustering analysis show a near-perfect separation of organs and developmental stages, for all three species (Supplementary Figure 6C, D). Chicken samples, which cluster apart from rodent samples in whole transcriptome analyses, are now grouped with the corresponding organs and developmental stages from mouse and rat. Our transcriptome collection can thus reveal highly conserved expression patterns for regulators of embryonic development, across amniotes.

Variations in transcriptome complexity among organs and developmental stages

We next sought to assess the transcriptome complexity in different organs across developmental stages. To predict lncRNAs, we used the RNA-seq data to reconstruct gene models with StringTie (Pertea et al. 2015), building on existing genomic annotations (Cunningham et al. 2019). We verified the protein-coding potential of newly annotated transcripts, based on the codon substitution frequency score (Lin et al. 2007, 2011) and on sequence similarity with known proteins, and we applied a stringent series of filters to reduce contaminations from un-annotated protein-coding UTRs and other artefacts (Materials and methods). We thus obtain a total of 18858 candidate lncRNAs in the mouse, 20159 in the rat and 5496 in the chicken, including both newly-annotated and previously known lncRNAs transcribed in our samples (Supplementary Dataset 1). The relative sizes of each species' lncRNA repertoires are consistent with previous studies (Necsulea et al. 2014; Sarropoulos et al. 2019). We note however that our power to detect lncRNAs in chicken is limited, due to the narrower organ and developmental stage sampling in this species (Supplementary Tables 1,2). Most candidate lncRNAs are expressed at very low levels. When imposing a minimum normalized expression level (transcript per million, or TPM) of 1, in at least one sample, the numbers of candidate lncRNAs falls to 12199, 15319 and 2892 in the mouse, rat and chicken, respectively (Supplementary Datasets 2, 3).

The differences in lncRNA content among species may be affected by RNA-seq read coverage and sample distribution, as well as genome sequence and annotation quality. To correct for the effect of RNA-seq read coverage, we down-sampled the RNA-seq data to obtain the same number of uniquely mapped reads for each organ/developmental stage combination within each species (Supplementary Methods). After this procedure, the number of detectable protein-coding genes (supported by at least 10 uniquely mapped reads) still shows broad variations among organs and developmental stages, with the highest numbers of genes detected in the testes, for all time points (Figure 2A). Large numbers of protein-coding genes (between approximately 12800 and 16700) are detected in all samples. In contrast, for lncRNAs, the pattern is much more striking: the young and aged adult testes express between 11000 and 12000 lncRNAs, in both mouse and rat, while in somatic organs and earlier developmental stages we can detect only between 1800 and 4800 lncRNAs (Figure 2B). This observation is in agreement with previous findings indicating that during spermatogenesis the chromatin environment is highly permissive to transcription (Soumillon et al. 2013).

Spatial and temporal expression patterns for protein-coding genes and lncRNAs

We next compared spatial and temporal expression patterns between protein-coding genes and lncRNAs. In agreement with previous findings (Soumillon et al. 2013), we show that lncRNAs are overwhelmingly preferentially expressed in the testes (Figure 3A). Indeed, more than 60% of lncRNAs reach their maximum expression level in this organ, compared to less than 35% of protein-coding

genes, for both mouse and rat (Figure 3A; Chi-square test p-value <$1e^{-10}$). Almost 80% of lncRNAs are preferentially expressed in young or aged adult samples, which is significantly higher than the fraction observed for protein-coding genes (less than 65%, Chi-square test p-value <$1e^{-10}$, Figure 3B).

We found that between 57% and 80% of protein-coding genes are significantly differentially expressed (DE) among developmental stages, at a false discovery rate (FDR) below 1%, in each organ and species (Figure 3C, Supplementary Dataset 4). The proportions of DE lncRNAs are significantly lower than the proportions of DE protein-coding genes in somatic organs, between 17% and 41% (Chi-square test, p-value <$1e^{-10}$). In the testes, we observed higher proportions of DE lncRNAs (63% in mouse and 67% in rat), but these values were still significantly lower than those observed for protein-coding genes (77% in mouse and 79% in rat; Chi-square test, p-value <$1e^{-10}$; Figure 3C). We suspected that the lower proportion of DE lncRNAs could be due to their low expression levels, as total read counts affect the sensitivity of DE tests (Anders and Huber 2010). Indeed, lncRNAs are expressed at much lower levels than protein-coding genes (Supplementary Figure 7). To control for this, we down-sampled the read counts observed for protein-coding genes, bringing them to the same average counts as lncRNAs but preserving relative gene abundance (Materials and methods). Strikingly, after down-sampling, we observe higher proportions of DE loci for lncRNAs compared to protein-coding genes (Figure 3C). The differences are statistically significant (Chi-square test, p-value <$1e^{-10}$) in all but one species / organ combination (mouse kidney, Chi-square test, p-value 0.15). We also observed that the expression amplitude among developmental stages are more important for lncRNAs than for protein-coding genes (Wilcoxon test, p-value <$1e^{-10}$, Supplementary Figure 8A), as expected given the lower lncRNA expression levels, which preclude detecting subtle expression shifts among time points. Finally, we observe that the developmental stage with maximum expression is generally different between protein-coding genes and lncRNAs, even when considering genes that are significantly DE among stages. For all organs, DE lncRNAs tend to show highest expression levels in the young and aged adults, while DE protein-coding genes are more homogeneously distributed among developmental stages (Chi-square test, p-value <$1e^{-10}$, Figure 3D, Supplementary Figure 8B).

Similar conclusions are reached when performing DE analyses between consecutive time points (Supplementary Figure 9, Supplementary Dataset 4). For both protein-coding genes and lncRNAs, the strongest expression changes are observed between newborn and young adult individuals. Almost 10000 lncRNAs are significantly up-regulated between newborn and young adult testes, confirming the strong enrichment for lncRNAs during spermatogenesis (Supplementary Figure 9). As expected, the lowest numbers of DE genes are observed at the transition between young and aged adult organs. At this time point, we observe more changes for the rat than for the mouse, potentially due to a higher proportion of immune cell infiltrates in the rat aged organ samples. Genes

associated with antigen processing and presentation tend to be expressed at higher levels in aged adults than in young adults, for mouse kidney, rat brain and liver (Supplementary Dataset 4).

Stronger selective constraint on lncRNAs expressed earlier in development

We next analyzed the long-term evolutionary sequence conservation for lncRNAs, in conjunction with their spatio-temporal expression patterns (Supplementary Table 5). We used the PhastCons score (Siepel et al. 2005) for placental mammals (Casper et al. 2018), to assess sequence conservation for various aspects of mouse lncRNAs: exons, promoters (defined as 400 bp regions upstream of the transcription start site), splice sites (first and last two bases of the introns). As approximately 20% of lncRNAs overlap with exonic regions on the opposite strand (Supplementary Dataset 1), we masked exonic regions from other genes before evaluating sequence conservation.

As previously observed (Ponjavic et al. 2007; Haerty and Ponting 2013), exonic and splice site sequence conservation is much lower for lncRNAs (median exonic score 0.094, median splice site score 0.075) than for protein-coding genes (median exonic score 0.42, median splice site score 0.85, Wilcoxon test p-value < $1e^{-10}$, Supplementary Figure 10). Exonic lncRNA conservation scores are significantly above the conservation observed for intergenic regions genome-wide (median score 0.076, Wilcoxon test, p-value < $1e^{-10}$, Supplementary Figure 10). Interestingly, intergenic regions found in the vicinity of lncRNA loci (Supplementary Methods) had slightly lower conservation scores than all intergenic regions, on average (median 0.072, Wilcoxon test, p-value < $1e^{-6}$, Supplementary Figure 10). Promoter conservation levels are more comparable between protein-coding genes (median score 0.17) and lncRNAs (median score 0.08), though still significantly higher for the former (Wilcoxon test, p-value < $1e^{-10}$, Supplementary Figure 10). Among lncRNA classes, the highest levels of promoter sequence conservation (median 0.14) are observed for bidirectional promoters shared with protein-coding genes (Supplementary Figure 10).

We next analyzed sets of protein-coding genes and lncRNAs that are expressed above noise levels (TPM>=1, averaged across all biological replicates) in each organ / developmental stage combination (Supplementary Table 6). For all examined regions and for both categories of genes, the spatio-temporal expression pattern is associated with the level of sequence conservation. Globally, sequence conservation is higher for genes that are expressed earlier in development than for genes expressed later in development, and reaches its lowest values for genes expressed in adult and aged testes (Figure 4). For exonic sequences and splice sites, the amount of sequence conservation is significantly lower for lncRNAs than for protein-coding genes, irrespective of the organ and developmental stage in which they are expressed (Wilcoxon test, p-value < $1e^{-10}$, Figure 4A, C). However, for promoter regions, the differences between the two gene categories are weaker, and are not statistically significant for the mid-stage embryonic brain (median 0.21 for protein-coding genes,

0.20 for lncRNAs, Wilcoxon test, p-value 0.08) and kidney (median 0.20 for protein-coding genes, 0.21 for lncRNAs, Wilcoxon test, p-value 0.76), and for the late embryonic kidney (median 0.20 for protein-coding genes, 0.19 for lncRNAs, Wilcoxon test, p-value 0.15). As noted before, the highest levels of lncRNA promoter conservation are observed for lncRNAs that have bidirectional promoters shared with protein-coding genes or other non-coding loci (Supplementary Figure 11A-C).

Finally, we asked whether the highest level of evolutionary sequence conservation is seen at exons, promoter or splice site regions, for lncRNA loci taken individually. Here again, the answer depends on the expression pattern: for lncRNAs detected in somatic organs and in the developing testes, there is significantly higher conservation for promoters than for exons (Wilcoxon test, p-value $< 1e^{-3}$ for all organ / developmental stage combinations, Supplementary Figure 11D, E). We also observe significantly higher conservation for splice sites than for exons (Wilcoxon test, p-value < 0.005), in all samples except aged liver (Wilcoxon test, p-value 0.052). However, when we consider lncRNAs that are expressed above noise levels in the young and aged adult testes (which constitute the great majority of loci), the conservation scores are slightly but significantly higher for exons than for promoters or splice sites (Wilcoxon test, p-value $< 1e^{-9}$, Supplementary Figure 11D, E).

Detection of homologous lncRNAs across species

We next sought to assess the conservation of lncRNA repertoires in mouse, rat and chicken. We detected lncRNA separately in each species, using only RNA-seq data and existing genome annotations, as previously suggested (Hezroni et al. 2015). We then searched for putative 1-to-1 orthologous lncRNAs between species using pre-computed whole-genome alignments as a guide (Materials and methods), to increase the sensitivity of orthologous gene detection in the presence of rapid sequence evolution (Washietl et al. 2014). The orthologous lncRNA detection procedure involves several steps, including the identification of putative homologous (projected) loci across species, filtering to remove large-scale structural changes in the loci, and intersection with predicted loci in the target species (Materials and methods). As illustrated in Figure 5, for comparisons between rodents the extent of sequence divergence is low enough that more than 90% of 18858 lncRNA loci are successfully projected from mouse to rat (Figure 5A, Supplementary Dataset 5). However, only 54% of projected loci have detectable transcription in the target species (at least 10 uniquely mapped reads). Only 23% of mouse lncRNA loci have predicted 1-to-1 orthologues in the rat, and only 15% are orthologous to confirmed lncRNA loci in the rat (Figure 5A, Supplementary Dataset 5). The 1493 mouse lncRNAs that have non-lncRNAs orthologues in the rat are generally matched with loci discarded because of low read coverage, minimum exonic length or distance to protein-coding genes (Supplementary Dataset 5). Cases of lncRNA-protein-coding orthologues are rare at this evolutionary distance (Supplementary Dataset 5), and they may stem from gene classification errors. We note that

orthologous lncRNA gene structures are highly divergent across species, in terms of exonic length or number of exons (Supplementary Figure 12). At larger evolutionary distances, the rate of sequence evolution is the main factor hampering detection of orthologous lncRNAs. Only 2613 (14%) of mouse lncRNAs could be projected on the chicken genome, and after subsequent filtering we detect only 66 mouse – chicken lncRNA orthologues, and 30 lncRNAs with orthologues in all three species (Supplementary Dataset 5, Supplementary Table 7).

Conserved lncRNAs differ from species-specific lncRNAs in terms of expression patterns. While only subtle differences can be observed when comparing mouse-rat orthologous lncRNAs to the mouse-specific lncRNA set, lncRNAs that are conserved between mouse and chicken are enriched in somatic organs and early developmental stages (Figure 5B, C). For example, only 15% of mouse-specific lncRNAs reach their maximum expression in the brain, which is significantly lower than the observed proportion for mouse lncRNAs with orthologues in rat (18%, Chi-square test, p-value $3e^{-4}$) and for mouse lncRNAs with orthologues in the chicken (39%, Chi-square test, p-value $1.5e^{-7}$). Likewise, while only 9.9% of mouse-specific lncRNAs have their highest level of expression in one of the two embryonic stages, this proportion is significantly higher for lncRNAs with orthologues in the chicken (27%, Chi-square test, p-value 0.002). We note however that these results may be affected by our narrower sampling for the chicken, which is biased towards embryonic organs, although we did include data from adult organs for this species (Supplementary Table 2).

Patterns of lncRNA expression variation across species, organs and developmental stages

We next assessed the global patterns of expression variation across species, organs and developmental stages, for predicted mouse – rat lncRNA orthologues (Supplementary Dataset 6). As for protein-coding genes, the main source of variability in a PCA performed on lncRNA expression levels is the difference between adult and aged testes and the other samples (Figure 6A). However, for lncRNAs, samples cluster according to the species of origin already on the second factorial axis (11.6% explained variance), confirming that lncRNA expression patterns evolve rapidly. Overall, differences between organs and developmental stages are less striking for lncRNAs, compared to differences between species (Figure 6A). This pattern is also visible on a hierarchical clustering analysis (performed on distances derived from Spearman's correlation coefficient): in contrast with what is observed for protein-coding genes, for lncRNAs samples generally cluster by species, with the exception of young and aged adult testes, which are robustly grouped (Figure 6B).

The higher rates of lncRNA expression evolution are also visible when analyzing within-species variations, through comparisons across biological replicates (Figure 7A). We sought to measure the selective pressures acting on expression patterns by contrasting between-species and within-species variations, in the spirit of a classical approach for coding sequences (McDonald and Kreitman 1991).

We constructed an expression conservation index by dividing the between-species and the within-species Spearman's correlation coefficient, computed on all genes from a category, for a given organ/developmental stage combination (Supplementary Methods). The resulting values are very high for protein-coding genes, in particular for the brain and the mid-stage embryonic kidney, where the expression conservation scores are above 0.95. However, there is significant less conservation between species for the adult and aged testes (expression conservation score ~0.88, bootstrap p-value <0.01, Figure 7B). For lncRNAs, expression conservation values vary between 0.5 and 0.7, significantly lower than for protein-coding genes (bootstrap p-value <0.01). The lowest conservation scores are observed for young and aged adult testes (Figure 7C).

Parallel patterns of temporal expression variation for mouse and rat lncRNAs

We delved deeper into the evolutionary comparison of protein-coding genes and lncRNA expression patterns, by asking whether temporal expression variations are shared between species. Several hundred orthologous lncRNAs are DE (FDR<0.01) in both mouse and rat, in each organ (minimum 150 in liver, maximum 1583 in testes, Figure 8A). Likewise, between 6775 (in liver) and 10608 (in testes) protein-coding genes are DE in both species (Supplementary Figure 13). Overall, shared DE lncRNAs show similar patterns of variation among developmental stages in mouse and rat, reaching their maximum expression in the same (or close) developmental stages (Figure 8A). For example, out of 42 lncRNAs that are DE in mouse brain and reach their maximum expression in the mid-stage embryo, 31 (74%) reach their maximum expression in the corresponding stage in the rat (Figure 8A). We clustered the relative expression profiles using the K-means algorithm (Supplementary Methods). Although individual gene trajectories show variations between species, the average expression profiles within each K-means cluster are generally similar between mouse and rat (Figure 8B-E, Supplementary Figure 13). This is particularly striking for the brain, where all 5 lncRNA clusters show similar average expression profiles for the two species (Figure 8B). Greater differences between species are observed in other organs, such as the kidney, where 2 out of 5 clusters (120 genes in total, that is 31% of shared DE lncRNAs in kidney) have average expression profiles that reach their maximum in different stages in mouse and rat (Figure 8C). The promoters of shared DE lncRNAs in each cluster contain transcription factor binding sites that are coherent with the expression profile of the cluster, such as brain homeobox POU3F2/BRN2 binding sites for the first K-means cluster in the brain, which has maximum expression in the mid-stage embryo (Supplementary Table 8). We note that transcription factor binding site enrichments are generally not statistically significant for lncRNAs, partly due to the low gene counts in each cluster.

The testis is the only organ where opposite K-mean cluster expression profiles are observed in the two species (increasing with time in mouse and decreasing in rat, or vice-versa). For lncRNAs, this

occurs for 1 of the 4 detected clusters, containing 56 lncRNAs (3.5% of all shared DE lncRNAs in this organ, Figure 8E). For protein-coding genes, opposite average profiles are observed for 2 out of 4 clusters, comprising 1182 and 1509 genes, i.e. 25% of all shared testes-DE protein-coding genes (Supplementary Figure 13). These clusters do not stand out in terms of transcription factor binding site (Supplementary Table 8) or gene ontology enrichment (Supplementary Dataset 4). This pattern confirms previous reports of rapid expression evolution in the adult testes (Brawand et al. 2011), and extends them by showing that patterns of variations among developmental stages are often species-specific in the testes, for protein-coding genes.

Evolutionary divergence of individual lncRNA expression profiles

To further quantify lncRNA expression differences between species, we measured the Euclidean distance between relative expression profiles (average TPM values across biological replicates, normalized by dividing by the sum of all values for a gene, for each species), for mouse and rat orthologues (Supplementary Methods, Supplementary Dataset 7, Supplementary Table 9). The resulting expression divergence values correlate negatively with the average expression level (R-squared 0.13, t-test p-value < $1e^{-10}$, Figure 9A), as expected given that abundance estimation is less reliable for weakly expressed genes. While the raw expression divergence values are significantly higher for lncRNAs (median 0.18) than for protein-coding genes (median 0.11, Wilcoxon test p-value < $1e^{-10}$, Figure 9B), this is largely due to the low lncRNA expression levels. Indeed, the effect disappears when analyzing the residual expression divergence after regressing the expression level (median value -0.03 for protein-coding genes, -0.06 for lncRNAs, Wilcoxon test < $1e^{-10}$, Figure 9C). These patterns remain true when analyzing separately protein-coding and lncRNAs with different types of promoters, bidirectional or unidirectional (Supplementary Figure 14A). For lncRNAs, we also observe a weak negative correlation between expression divergence and the extent of gene structure conservation (R-squared 0.04, t-test p-value < $1e^{-10}$, Figure 9D). We measured the relative contribution of each organ/developmental stage to the expression divergence estimate (Figure 9E). For both protein-coding genes and lncRNAs, by far the highest contributors are the young adult and aged testes samples, which are responsible for almost 30% of the lncRNA expression divergence (Figure 9E). This is visible in the expression patterns of the 2 protein-coding and lncRNA genes with the highest residual expression divergence: the lncRNA expression divergence is mostly due to changes in adult testes, while more complex expression pattern changes seem to have occurred for the protein-coding genes (Supplementary Figure 14). The most divergent protein-coding genes are enriched in functions related to immunity (Supplementary Dataset 7), suggesting that differences in immune cell infiltrates among species could be responsible for these extreme cases of expression pattern divergence.

Candidate species-specific lncRNAs

We next investigated the most extreme cases of expression divergence: situations where expression can be robustly detected in one species, but not in the other one, despite almost perfect sequence alignment (Supplementary Methods). We selected lncRNA loci that were supported by at least 100 uniquely mapped reads in one species, with no reads detected in the predicted homologous region in the other species. With this convention, we obtain 1041 candidate mouse-specific and 1646 candidate rat-specific loci (Supplementary Dataset 8). These lists include striking examples, such as the region downstream of the *Fzd4* protein-coding gene, which contains a mouse-specific and a rat-specific lncRNA candidate, each perfectly aligned in the other species (Supplementary Figure 15). Candidate species-specific lncRNAs are more frequently associated with predicted enhancers than orthologous lncRNAs (52% vs. 33%, Chi-square test, p-value $<1e^{-10}$), are less often spliced (56% vs. 61%, Chi-square test p-value $1.6e^{-3}$) and associated with bidirectional promoters (24% vs. 61%, Chi-square test, p-value $<1e^{-10}$, Supplementary Figure 16). Moreover, we could confirm that their presence is associated with increased expression divergence in the neighboring genes. To test this, we selected species-specific and orthologous lncRNAs that are transcribed from bidirectional promoters shared with protein-coding genes, and evaluated the expression divergence of their protein-coding neighbors (Supplementary Figure 16D, E). Though the difference is subtle, genes that are close to species-specific lncRNAs have significantly higher expression divergence than the ones that have conserved lncRNA neighbors, even after correcting for expression levels (Wilcoxon test, p-value $< 1e^{-3}$). It thus seems that expression changes that led to the species-specific lncRNA transcription extend beyond the lncRNA locus and affect neighboring genes, as previously proposed (Kutter et al. 2012).

Discussion

Comparative transcriptomics across species, organs and developmental stages

More than a decade after the publication of the first genome-wide lncRNA datasets (Guttman et al. 2009; Khalil et al. 2009), the debate regarding their functionality is still not settled. Evolutionary approaches provide important tools to assess biological functionality (Haerty and Ponting 2014), and they have been already successfully applied to lncRNAs. However, most large-scale comparative transcriptomics studies available so far (Kutter et al. 2012; Washietl et al. 2014; Hezroni et al. 2015; Necsulea et al. 2014), with one recent exception (Sarropoulos et al. 2019), have focused on lncRNAs detected in adult organs. We hypothesized that lncRNAs expressed during development may be enriched in functional loci, as suggested by the increasing number of lncRNAs with proposed developmental roles (Rinn et al. 2007; Sauvageau et al. 2013; Grote et al. 2013; Grote and Herrmann 2015). To test this hypothesis, we performed a multi-dimensional comparative transcriptomics analysis, following lncRNA and protein-coding genes across species, organs and developmental stages.

We ensured that our transcriptome collection reflects the changes in cellular composition and physiological functions that occur during major organ development, by analyzing cell-type specific gene markers derived from single-cell analyses (Tabula Muris Consortium 2018; Green et al. 2018). We showed that protein-coding gene expression profiles across major organs and developmental stages are well conserved among species, even at large evolutionary distances. Although differences among rodents and chicken are considerable when analyzing the full set of orthologous protein-coding genes (Figure 1), the expression profiles of genes that are known to be implicated in embryonic development and in gene expression regulation processes are highly conserved among species (Supplementary Figure 6). Our transcriptome collection thus enables detecting temporal expression patterns shared across divergent species, for key players in developmental regulatory networks. These observations are consistent with findings from a recent publication, which studied protein-coding gene expression patterns during major organ development in amniote species (Cardoso-Moreira et al. 2019). Our transcriptome dataset covers a narrower range of species and developmental stages than this comprehensive resource (Cardoso-Moreira et al. 2019), but uniquely includes aged individuals, thus completing the overview of temporal expression patterns. Thus, our work represents an additional resource for evolutionary studies of gene expression.

To our knowledge, together with a recent publication (Sarropoulos et al. 2019), our work is one of the first large-scale lncRNA evolutionary studies that include a temporal dimension, by sampling different developmental stages. Our manuscript and this recent work concur to reveal an enrichment for functional lncRNAs early in development (Sarropoulos et al. 2019). Here, we perform in-depth analyses of expression pattern evolution, short-term and long-term sequence evolution for different regions of lncRNAs loci, in conjunction with their expression patterns. We thus bring new insights into the evolution and functionality of lncRNAs.

Spatio-temporal lncRNA expression patterns

Our first major observation is that lncRNAs are overwhelmingly expressed in the young and aged adult testes (Figure 3), in agreement with previous data (Soumillon et al. 2013). Their relative depletion in embryonic and newborn testes reinforces the association between lncRNA transcription and spermatogenesis, in accord with the hypothesis that the particular chromatin environment during spermatogenesis is a driver for promiscuous, non-functional transcription (Kaessmann 2010; Soumillon et al. 2013). Interestingly, we show that lncRNAs are significantly differentially expressed among developmental stages, at least as frequently as protein-coding genes, after correcting for their lower expression levels. However, in contrast with protein-coding genes, the majority of lncRNAs reach their highest expression levels in adult rather than in developing organs (Figure 3). As requirements for tight gene expression control are higher during embryonic development (Ben-Tabou de-Leon and

Davidson 2007), an explanation for the relative lncRNA depletion in embryonic and newborn transcriptomes is that transcriptional noise is deleterious and thus more efficiently blocked during the early stages of development. Differences in cellular composition heterogeneity may also be part of the explanation. Expression analyses of cell-type specific markers suggest that adult organ transcriptomes may be a mix of more diverse cell types, including substantial immune cell infiltrates (Supplementary Figure 1). A higher cell type diversity may explain the increased abundance of lncRNAs in young and aged adult organs, especially given that lncRNAs are thought to be cell-type specific (Liu et al. 2016).

We found that lncRNA expression patterns are generally similar between young and aged adult individuals: less than 50 lncRNAs are significantly DE between these two stages, for most organs (Supplementary Figure 9). Moreover, the levels of sequence and expression conservation are globally similar between young and aged adults, for both protein-coding and lncRNA genes (Figures 4,7). Overall, our analyses indicate that, with our sampling (Supplementary Table 1), the physiological processes at work in aged organs are highly similar to those acting in juvenile organs, suggesting that developmental stage sampling should be further extended for in-depth analyses of the aging process.

Functionally constrained lncRNAs are enriched in developmental transcriptomes

Our long-term sequence conservation analyses confirm that lncRNAs are overall under weak, but significant selective constraint (Ponjavic et al. 2007): lncRNA sequence conservation scores are much lower than those of protein-coding genes, but above those of intergenic regions (Figure 4, Supplementary Figures 10-11). Interestingly, intergenic regions flanking lncRNAs are on average less conserved than the genomic intergenic average (Figure 4), suggesting that the rapid lncRNA evolution may be a general feature of the genomic regions in which they reside. The underlying mechanisms are unclear, but may reflect a lower density of constrained expression regulatory elements in the vicinity of lncRNAs, or a higher accumulation of lineage-specific transposable elements (Kapusta et al. 2013).

We show that, for those lncRNAs that are expressed above noise levels (TPM>=1) in somatic organs and in the embryonic and newborn developmental stages, there is a higher proportion of evolutionarily constrained loci than in testes-expressed lncRNAs (Figure 4). Strikingly, we find that the level of long-term sequence conservation for lncRNA promoter regions is similar to the one observed for protein-coding promoters, when we analyze genes that are robustly expressed in embryonic brain and kidney. Furthermore, we show that lncRNAs expressed in somatic organs and in the developing testes differ from those expressed in the adult testes not only in terms of overall levels of sequence conservation, but also with respect to the regions of the lncRNA loci that are under selective constraint. Thus, for lncRNAs expressed in somatic organs and in the developing testes, there is significantly more evolutionary constraint on promoters and splice sites than on exons, while these patterns are not seen for the bulk of lncRNAs, expressed in adult and aged testes (Supplementary Figure 11). We are thus

able to modulate previous reports of increased constraint on splicing regulatory regions in mammalian lncRNAs (Schüler et al. 2014; Haerty and Ponting 2015), by showing that this pattern is specific to lncRNAs that are expressed in somatic organs and in the developing testes.

These results are also in agreement with recent findings suggesting that biological function may reside in the presence of additional non-coding regulatory elements at the lncRNA promoter rather than in the production of a specific transcript (Engreitz et al. 2016; Groff et al. 2016). While the elevated sequence conservation at splicing regulatory signals could indicate that the production of a specific mature lncRNA is required, splicing of lncRNA transcripts was recently proposed to affect the expression of neighboring protein-coding genes (Engreitz et al. 2016). Thus, while there is evidence for increased functionality for lncRNA loci that are detected in developmental transcriptomes or in adult somatic organs, in agreement with a recent report (Sarropoulos et al. 2019), our sequence conservation analyses are compatible with the hypothesis that their biological functions may be carried out in an RNA-independent manner, as exons are under less constraint than promoters or splice sites. Alternatively, their function may be carried out by small conserved elements, such that the sequence conservation on the entire lncRNA exonic sequence is weak (Ulitsky 2016).

Evolutionary divergence of spatio-temporal expression profiles for lncRNAs

We previously showed that lncRNA expression patterns evolve rapidly across species in adult organs (Necsulea et al. 2014). Here, we show that this rapid evolution of lncRNA expression is also true for embryonic and newborn developmental stages. Expression comparisons across species, organs and developmental stages are dominated by differences between species for lncRNAs (Figure 6), while similarities between organs and developmental stages are predominant for protein-coding genes, even across distantly-related species (Figure 1). We assessed the extent of expression conservation by contrasting between-species and within-species expression variations and we showed that lncRNAs have significantly lower levels of conservation than protein-coding genes, for all organs and developmental stages (Figure 7). However, lncRNA expression is more conserved in somatic organs and in early embryonic stages than in the adult testes. Moreover, when orthologous lncRNAs are differentially expressed among developmental stages in both mouse and rat, they generally show parallel profiles of expression variation in both species (Figure 8). This result is in agreement with a recent publication, which showed that temporal patterns of expression variation tend to be evolutionarily conserved for developmentally dynamic lncRNAs (Sarropoulos et al. 2019). We note that these temporal patterns of variation may in fact be caused by spatially-restricted lncRNA expression. Previous reports indicated that lncRNA expression may be cell type-specific (Liu et al. 2016). The differentially expressed lncRNAs, shared across mouse and rat, could be specific of cell types that change their relative abundance in whole-organ transcriptomes with developmental time.

572 Interestingly, when we evaluate expression divergence individually for each orthologous gene
573 pair, correcting for the lower lncRNA expression levels, we find that lncRNAs are not more divergent
574 than protein-coding genes (Figure 8). This observation indicates that much of the between-species
575 differences in lncRNA expression patterns is tightly linked with the low expression levels of lncRNAs. It
576 is not clear however whether this is purely an indication of technical biases, that hamper expression
577 estimation for lowly expressed lncRNAs, or whether the low lncRNA expression levels are a sign that
578 these transcripts are non-functional. For cell type-specific lncRNAs, low expression in whole-organ
579 transcriptomes are expected. This question may soon be directly addressed, as single-cell assays
580 become more sensitive and allow investigation of lncRNAs (Liu et al. 2016).

581 *Candidate species-specific lncRNAs*

582 Finally, we analyzed extreme cases of expression divergence between species, where
583 transcription can be robustly detected in one species but not in the other, despite the presence of
584 good sequence conservation. We identify more than a thousand candidate species-specific lncRNAs,
585 in both mouse and rat. Interestingly, we observe that candidate mouse-specific lncRNAs are more
586 frequently transcribed from enhancers than lncRNAs conserved between mouse and rat
587 (Supplementary Figure 11). This observation is consistent with previous reports that enhancers and
588 enhancer-associated lncRNAs evolve rapidly (Villar et al. 2015; Marques et al. 2013). Moreover, we
589 show that these lncRNA expression changes do not occur in an isolated manner. When species-specific
590 lncRNA transcription was inferred at protein-coding genes bidirectional promoters, the neighboring
591 protein-coding genes also showed increased expression divergence, compared to genes that are
592 transcribed from conserved lncRNA promoters. We thus confirm that lncRNA turnover is associated
593 with changes in neighboring gene expression (Kutter et al. 2012). While lncRNAs changes may be
594 directly affecting gene expression, another probable hypothesis is that a common mechanism affects
595 both lncRNAs and protein-coding genes transcribed from bidirectional promoters.

596 *Conclusions*

597 Our comparative transcriptomics approach confirms that lncRNAs repertoires, sequences and
598 expression patterns evolve rapidly across species, and shows that accelerated rates of lncRNA
599 evolution are also seen in developmental transcriptomes, albeit less frequently. These observations
600 are consistent with the hypothesis that the majority of lncRNAs (or at least of those detected with
601 sensitive transcriptome sequencing approaches, in particular in the adult testes) may be non-
602 functional. However, we are able to modulate this conclusion, by showing that there are increased
603 levels of functional constraint on lncRNAs expressed during embryonic development, in particular in
604 the developing brain and kidney. These increased levels of constraint apply to all analyzed aspects of
605 lncRNAs, including sequence conservation for exons, promoter and splice sites, but also expression

pattern conservation. For many of these loci, biological function may be RNA-independent, as the highest levels of selective constraint are observed on promoter regions and on splice signals, rather than on lncRNA exonic sequences. Our results are thus compatible with unconventional, RNA-independent functions for lncRNAs expressed during embryonic development.

Materials and methods

Biological sample collection

We collected samples from three species (mouse C57BL/6J strain, rat Wistar strain and chicken White Leghorn strain), four organs (brain, kidney, liver and testes) and five developmental stages (including two embryonic stages, newborn, young and aged adult individuals). We sampled the following stages in the mouse: embryonic day post-conception (dpc) 13.5 (E13.5 dpc, hereafter mid-stage embryo); E17 to E17.5 dpc (late embryo); post-natal day 1 to 2 (newborn); young adult (8-10 weeks old); aged adult (24 months old). For the rat, we sampled the following stages: E15 dpc (mid-stage embryo); E18.5 to E19 dpc (late embryo); post-natal day 1 to 2 (newborn); young adult (8-10 weeks old); aged adult (24 months, with the exception of kidney samples and two of four liver samples, derived from 12 months old individuals). The embryonic and neonatal developmental stages were selected for maximum comparability based on Carnegie stage criteria (Theiler 1989). For chicken, we collected samples from Hamburger-Hamilton stages 31 and 36 (hereafter termed mid-stage and late embryo), selected for comparability with the two embryonic stages in mouse and rat (Hamburger and Hamilton 1951). Each sample corresponds to one individual, except for mouse and rat mid-stage embryonic kidney, for which tissue from several embryos was pooled prior to RNA extraction. For adult and aged organs, multiple tissue pieces from the same individual were pooled and homogenized prior to RNA extraction. For brain dissection, we sampled the cerebral cortex. For mouse and rat, with the exception of the mid-stage embryonic kidney, individuals were genotyped and males were selected for RNA extraction. Between two and four biological replicates were obtained for each species/organ/stage combination, amounting to 97 samples in total (Supplementary Table 1).

RNA-seq library preparation and sequencing

We performed RNA extractions using RNeasy Plus Mini kit from Qiagen. We assessed RNA quality with the Agilent 2100 Bioanalyzer. RNA integrity numbers (RIN) are available in Supplementary Table 1; see Supplementary Methods for additional RNA integrity analyses. Sequencing libraries were produced with the Illumina TruSeq stranded mRNA protocol with polyA selection, and sequenced as 101 base pairs (bp) single-end reads, at the Genomics Platform of iGE3 and the University of Geneva. Libraries are strand-specific and the sequenced strand is complementary to the RNA molecule.

Additional RNA-seq data

To improve detection power for lowly expressed lncRNAs, we complemented our RNA-seq collection with samples generated with the same technology for Brown Norway rat adult organs (Cortez et al. 2014). We added published data for adult chicken (red jungle fowl strain UCD001) organs (McCarthy et al. 2019), as well as for embryonic chicken (White Leghorn) organs (Uebbing et al. 2015; Ayers et al. 2013). As the data were not comparable with our own in terms of library preparation and animal strains, these samples were only used to increase lncRNA detection sensitivity.

RNA-seq data processing

We used HISAT2 (Kim et al. 2015) release 2.0.5 to align the RNA-seq data on reference genomes. The genome sequences (assembly versions mm10/GRCm38, rn6/Rnor_6.0 and galGal5/Gallus_gallus-5.0) were downloaded from the Ensembl database (Cunningham et al. 2019). Genome indexes were built using only genome sequence information. To improve detection sensitivity, at the alignment step we provided known splice junction coordinates extracted from Ensembl. We set the maximum intron length for splice junction detection at 1 million base pairs (Mb). The following command-line arguments were used: --rna-strandness R –known-splicesite-infile=SpliceSites_Ensembl.txt --max-intronlen 1000000 --dta-cufflinks, where SpliceSites_Ensembl.txt corresponds to the exon junction coordinates extracted with hisat2_extract_splice_sites.py. See also Supplementary Methods for additional RNA-seq data quality analyses.

Transcript assembly and filtering

We assembled transcripts for each sample using StringTie (Pertea et al. 2015), release 1.3.5, based on read alignments obtained with HISAT2. We provided genome annotations from Ensembl release 94 as a guide for transcript assembly. We filtered Ensembl annotations to remove transcripts that spanned a genomic length above 2.5 Mb. For protein-coding genes, we kept only protein-coding transcripts, discarding isoforms annotated as “retained_intron”, “processed_transcript” etc. We set the minimum exonic length at 150 bp, the minimum anchor length for splice junctions at 8bp and the minimum isoform fraction at 0.05. The following StringTie command-line arguments were used: -G Ensembl_annotations.gtf -m 150 -a 8 -f 0.05 –p 8 –rf, where Ensembl_annotations.gtf correspond to the Ensembl annotations filtered as described above. We compared the resulting assembled transcripts with Ensembl annotations and we discarded read-through transcripts, overlapping with multiple multi-exonic Ensembl-annotated genes. For strand-specific samples, we discarded transcripts for which the ratio of sense to antisense unique read coverage was below 0.01. We discarded multi-exonic transcripts that were not supported by splice junctions with correctly assigned strands. The filtered transcripts obtained for each sample were assembled into a single dataset *per* species using the merge option in StringTie. For increased sensitivity, we removed the minimum FPKM and TPM

thresholds, but required a minimum isoform fraction of 0.05 for transcript inclusion. The following StringTie command-line arguments were used: stringtie -v --merge -G Ensembl_annotations.gtf -m 150 -a 8 -p 8 -F 0 -T 0 -f 0.05. We constructed a combined annotation dataset, starting with Ensembl annotations, to which we added newly-assembled transcripts that had no exonic overlap with Ensembl genes. We also included newly-annotated isoforms for known genes if they had exonic overlap with exactly one Ensembl gene, thus discarding potential read-through transcripts or gene fusions.

Protein-coding potential of assembled transcripts

To determine whether the newly assembled transcripts were protein-coding or non-coding, we mainly relied on the codon substitution frequency (CSF) score (Lin et al. 2007). As in a previous publication (Necsulea et al. 2014) we scanned whole genome alignments and computed CSF scores in 75 bp sliding windows moving with a 3 bp step. We used pre-computed alignments downloaded from the UCSC Genome Browser (Casper et al. 2018), including the alignment between the mouse genome and 59 other vertebrates (for mouse classification), between the human genome and 99 other vertebrates (for rat and chicken classification) and between the rat genome and 19 other vertebrates (for rat classification). For each window, we computed the score in each of the 6 possible reading frames and extracted the maximum score for each strand. We considered that transcripts are protein-coding if they overlapped with positive CSF scores on at least 150 bp. As positive CSF scores may also appear on the antisense strand of protein-coding regions due to the partial strand-symmetry of the genetic code, in this analysis we considered only exonic regions that did not overlap with other genes. In addition, we searched for sequence similarity between assembled transcripts and known protein sequences from the SwissProt 2017_04 (The UniProt Consortium 2017) and Pfam 31.0 (El-Gebali et al. 2019) databases. We kept only SwissProt entries with confidence scores 1, 2 or 3 and we used the Pfam-A curated section of Pfam. We searched for sequence similarity using the blastx utility in the BLAST+ 2.8.1 package (Camacho et al. 2009; Altschul et al. 1990), keeping hits with maximum e-value $1e^{-3}$ and minimum protein sequence identity 40%, on repeat-masked cDNA sequences. We considered that transcripts were protein-coding if they overlapped with blastx hits over at least 150 bp. Genes were said to be protein-coding if at least one of their isoforms was classified as protein-coding, based on either the CSF score or on sequence similarity with known proteins.

Long non-coding RNA selection

To construct a reliable lncRNA dataset, we selected newly-annotated genes classified as non-coding based on both the CSF score and on sequence similarity with known proteins and protein domains, as well as Ensembl-annotated genes with non-coding biotypes (“lincRNA”, “processed_transcript”, “antisense”, “TEC”, "macro_lncRNA", "bidirectional_promoter_lncRNA", "sense_intronic"). For newly detected genes, we applied several additional filters: we required a

minimum exonic length (corresponding to the union of all annotated isoforms) of at least 200 bp for multi-exonic loci and of at least 500 bp for mono-exonic loci; we eliminated genes that overlapped for more than 5% of their exonic length with unmappable regions; we kept only loci that were classified as intergenic and at least 5 kb away from Ensembl-annotated protein-coding genes on the same strand; for multi-exonic loci, we required that all splice junctions be supported by reads with correct strand assignment (cf. above). For both *de novo* and Ensembl annotations, we removed transcribed loci that overlapped on at least 50% of their length with retrotransposed gene copies, annotated by the UCSC Genome Browser and from a previous publication (Carelli et al. 2016); we discarded loci that overlapped with UCSC-annotated tRNA genes and with RNA-type elements from RepeatMasker (Smit et al. 2003) on at least 25% of their length. We kept loci supported by at least 10 uniquely mapped RNA-seq reads and for which a ratio of sense to antisense transcription of at least 1% was observed in at least one sample. Although the fraction of reads stemming from the wrong strand due to errors in library preparations is very low in our samples (Supplementary Table 1), loci situated on the antisense strand of highly expressed genes can have unreliable expression estimates. Thus, for loci that had sense/antisense exonic overlap with other genes, we computed expression levels either on complete gene annotations, or only on exonic regions that had no overlap with other genes, and computed Spearman's correlation coefficient between the two expression estimates, across all samples. We discarded loci for which the correlation coefficient was below 0.9. Full gene annotations and lncRNA selection criteria are provided in Supplementary Dataset 1 online.

Gene expression estimation

We computed the number of uniquely mapping reads unambiguously attributed to each gene using the Rsubread package in R (Liao et al. 2019), discarding reads that overlapped with multiple genes. We also estimated read counts and TPM (transcript *per* million) values *per* gene using Kallisto (Bray et al. 2016). To approach absolute expression levels estimates, for better comparisons across samples, we further normalized TPM values using a scaling approach (Brawand et al. 2011). Briefly, we ranked the genes in each sample according to their TPM values, we computed the variance of the ranks across all samples for each gene, and we identified the 100 least-varying genes, found within the inter-quartile range (25%-75%) in terms of average expression levels across samples. We derived normalization coefficients for each sample such that the median of the 100 least-varying genes be identical across samples. We then used these coefficients to normalize TPM values for each sample. We excluded mitochondrial genes from expression estimations and analyses, as these genes are highly expressed and can be variable across samples. For differential expression analyses, we used *per*-gene unique read counts computed with Rsubread. For all downstream analyses we used normalized TPM

values. When indicated, we transformed TPM values with the following formula: x->log2(x+1). Gene expression data is available in Supplementary Dataset 2 online.

Differential expression analyses

We used the DESeq2 (Love et al. 2014) package release 1.22.2 in R release 3.5.0 (R Core Team 2018) to test for differential expression across developmental stages, separately for each organ and species. We analyzed both protein-coding genes and lncRNAs, selected according to the criteria described above. We first performed a global differential expression analysis, using the likelihood ratio test to contrast a model including an effect of the developmental stage against the null hypothesis of homogeneous expression across all developmental stages. This analysis was performed on all protein-coding and lncRNA genes for each species, as well as on 1-to-1 orthologues for mouse and rat. In addition, we down-sampled the numbers of reads assigned to protein-coding genes to obtain identical average numbers of reads for protein-coding genes and lncRNAs. The resampled read counts were directly proportional to the original counts for each protein-coding gene. We also contrasted consecutive developmental stages, for each species and organ, using the Wald test implemented in DESeq2. Differential expression results are available in Supplementary Dataset 4 online.

Homologous lncRNA family prediction

We used existing whole-genome alignments as a guide to predict homologous lncRNAs across species, as previously proposed (Washietl et al. 2014). We first constructed for each gene the union of its exon coordinates across all isoforms, hereafter termed “exon blocks”. We projected exon block coordinates between pairs of species using the liftOver utility and whole-genome alignments generated with blastz (http://www.bx.psu.edu/miller_lab/), available through the UCSC Genome Browser (Casper et al. 2018). To increase detection sensitivity, for the initial liftOver projection we required only that 10% of the reference bases remap on the target genome. Projections were then filtered, retaining only cases where the size ratio between the projected and the reference region was between 0.33 and 3 for mouse and rat (0.2 and 5 for comparisons involving chicken). To exclude recent lineage-specific duplications, regions with ambiguous or split liftOver projections were discarded. For genes where multiple exon blocks could be projected across species, we defined the consensus chromosome and strand in the target genome and discarded projected exon blocks that did not match this consensus. We then evaluated the order of the projected exon blocks on the target genes, to identify potential internal rearrangements. If internal rearrangements were due to the position of a single projected exon block, the conflicting exon block was discarded; otherwise, the entire projected gene was eliminated. As the projected reference gene coordinates could overlap with multiple genes in the target genome, we constructed gene clusters based on the overlap between projected exon block coordinates and target annotations, using a single-link clustering approach. We then realigned

entire genomic loci for each pair of reference-target genes found within a cluster, using lastz (http://www.bx.psu.edu/miller_lab/) and the threaded blockset aligner TBA (Blanchette et al. 2004). Using this alignment, we computed the percentage of exonic sequences aligned without gaps and the percentage of identical exonic sequence, for each pair of reference-target genes. We then extracted the best hit in the target genome for each gene in the reference genome based on the percentage of identical exonic sequence, requiring that the ratio between the maximum percent identity and the percent identity of the second-best hit be above 1.1. Reciprocal best hits were considered to be 1-to-1 orthologous loci between pairs of species. For analyses across all three species, we constructed clusters of reciprocal best hits from pairwise species comparisons, using a single-link clustering approach. Resulting clusters with more than 1 representative *per* species were discarded. The results of the homology prediction pipeline, sequence alignment statistics and Ensembl orthology relationships for protein-coding genes are available in Supplementary Dataset 5 online.

Availability of data and materials

The RNA-seq data were submitted to the NCBI Gene Expression Omnibus (GEO), under accession number GSE108348. Supplementary Datasets containing additional processed data are available at the address: ftp://pbil.univ-lyon1.fr/pub/datasets/Darbellay_LncEvoDevo

The scripts used to analyse the data are available through a GitHub repository: https://github.com/anecsulea/LncEvoDevo . See also Supplementary Methods.

Author contributions

FD performed organ dissections, RNA extractions, quality control, prepared samples for sequencing and contributed to study design and manuscript preparation. AN designed the study, performed computational analyses and wrote the manuscript.

Acknowledgements

We thank Denis Duboule and all members of the laboratory for advice and support, Mylène Docquier, Brice Petit and the Genomics Platform of the University of Geneva for RNA-seq data production, Amanda Cooksey and the Chickspress Team at the University of Arizona (http://geneatlas.arl.arizona.edu) for granting us access to chicken RNA-seq data, Ioannis Xenarios and the Vital-IT team for computational support. We thank Jean-Marc Matter (University of Geneva) for providing chicken eggs. This work was performed using the computing facilities of the CC LBBE/PRABI, the Vital-IT Center for high-performance computing of the SIB Swiss Institute of Bioinformatics (http://www.vital-it.ch) and the computing center of the French National Institute of Nuclear and Particle Physics (CC-IN2P3). This project was funded by the Swiss National Science Foundation (SNSF Ambizione grant PZ00P3_142636), the Agence Nationale pour la Recherche (ANR JCJC 2017 LncEvoSys). FD was supported by a FP7 IDEAL grant (259679).

Figure legends

Figure 1. Comparative transcriptomics across species, organs and developmental stages.

A. Experimental design. The developmental stages selected for mouse, rat and chicken are marked on a horizontal axis. Organs sampled for each species and developmental stage are shown below. Abbreviations: br, brain; kd, kidney; lv, liver; ts, testes.

B. First factorial map of a principal component analysis, performed on log2-transformed TPM values, for 10,363 protein-coding genes with orthologues in mouse, rat and chicken. Colors represent different organs and developmental stages, point shapes represent different species.

C. Hierarchical clustering, performed on a distance matrix derived from Spearman correlations between pairs of samples, for 10,363 protein-coding genes with orthologues in mouse, rat and chicken. Organ and developmental stages are color-coded, shown below the heatmap. Species of origin is color-coded, shown on the right. Sample clustering is shown on the left.

Figure 2. Transcriptome complexity in different species, organs and developmental stages.

A. Number of protein-coding genes supported by at least 10 uniquely mapped reads in each sample, after read resampling to homogenize coverage (Supplementary Methods). Colors represent different organs, point shapes represent different species. Developmental stages are indicated by numeric labels, 1 to 5, on the X-axis. We analyzed a total of 19,356 protein-coding genes in the mouse, 19,274 in the rat and 15,509 in the chicken.

D. Number of lncRNAs supported by at least 10 uniquely mapped reads in each sample, after read resampling to homogenize coverage. We analyzed a total of 18,858 candidate lncRNAs in the mouse, 20,159 in the rat and 5,496 in the chicken.

Figure 3. Different expression patterns for protein-coding genes and lncRNAs.

A. Distribution of the organ in which maximum expression is observed, for protein-coding genes (pc) and lncRNAs (lnc), for mouse, rat and chicken. Organs are color-coded, shown above the plot. We defined the sample in which maximum expression is observed based on average expression values across replicates, for each organ / developmental stage combination (Supplementary Methods).

B. Distribution of the developmental stage in which maximum expression is observed, for protein-coding genes and lncRNAs, for mouse, rat and chicken. Developmental stages are color-coded, shown above the plot.

C. Percentage of protein-coding and lncRNA genes that are significantly (FDR<0.01) differentially expressed (DE) among developmental stages, with respect to the total number of genes tested for each organ. Left panel: differential expression analysis performed with all RNA-seq reads.

Right panel: differential expression analysis performed after down-sampling read counts for protein-coding genes, to match those of lncRNAs (Materials and methods).

D. Distribution of the developmental stage in which maximum expression is observed, for protein-coding genes and lncRNAs that are significantly DE (FDR<0.01) in each organ, for the mouse. Percentages are computed with respect to the total number of DE genes in each organ and gene class.

Figure 4. Increased levels of long-term sequence conservation for lncRNAs expressed early in development.

A. Sequence conservation scores (PhastCons scores, placental mammals) for protein-coding and lncRNAs exonic regions, for subsets of genes expressed above noise levels (TPM>=1) in each organ and developmental stage. Dots represent medians, vertical bars represent 95% confidence intervals. Numbers of analyzed genes are provided in Supplementary Table 5. Organs are color-coded; developmental stages are indicated (numbers 1 to 5) on the X-axis. The gray dots and vertical bars represent the median value and 95% confidence interval for all intergenic regions, genome-wide, or for intergenic regions flanking lncRNA loci (Supplementary Methods).

B. Same as A, for promoter regions (400 bp upstream of transcription start sites). Exonic sequences were masked before assessing conservation.

C. Same as B, for splice sites (first and last two bases of each intron).

Figure 5. Orthologous lncRNA families for mouse, rat and chicken.

A. Number of mouse protein-coding genes and lncRNAs in different classes of evolutionary conservation. From left to right: all loci, loci with conserved sequence in the rat, loci for which transcription could be detected (at least 10 unique reads) in predicted orthologous locus in the rat, loci with predicted 1-to-1 orthologues, loci for which the predicted orthologue belonged to the same class (protein-coding or lncRNA) in the rat, loci with conserved sequence in the chicken, loci for which transcription could be detected (at least 10 unique reads) in predicted orthologous locus in the chicken, loci with predicted 1-to-1 orthologues, loci for which the predicted orthologue belonged to the same class (protein-coding or lncRNA) in the chicken. We analyze 19,356 protein-coding genes and 18,858 candidate lncRNAs in the mouse.

B. Distribution of the organ in which maximum expression is observed, for mouse protein-coding and lncRNA genes that have no orthologues in the rat or chicken, for genes with orthologues in the rat and for genes with orthologues in chicken. The sample in which maximum expression is observed is computed based on average expression values across biological replicates, for each organ / developmental stage combination (Supplementary Methods).

C. Same as B, for the distribution of the developmental stage in which maximum expression is observed.

Figure 6. Global comparison of lncRNA expression patterns across species.

A. First factorial map of a principal component analysis, performed on log2-transformed TPM values, for 2,893 orthologous lncRNAs between mouse and rat. Colors represent different organs and developmental stages, point types represent species.

B. Hierarchical clustering, performed on a distance matrix derived from Spearman correlations between pairs of samples, for 2,893 orthologous lncRNAs between mouse and rat. Organ and developmental stages are shown below the heatmap. Species of origin is shown on the right. Sample clustering is shown on the left.

Figure 7. Global estimates of expression conservation across organs and developmental stages.

A. Example of between-species and within-species variation of expression levels, for protein-coding genes (left) and lncRNAs (right), for orthologous genes between mouse and rat, for the mid-stage embryonic brain. Spearman's correlation coefficients (rho) are shown above each plot. We show a smoothed color density representation of the scatterplots, obtained through a 2D kernel density estimate (smoothScatter function in R).

B. Expression conservation index, defined as the ratio of the between-species and the within-species expression level correlation coefficients, for protein-coding genes, for each organ and developmental stage. The vertical segments represent minimum and maximum values obtained from 100 bootstrap replicates. We analyzed 15,931 pairs of orthologous protein-coding genes.

C. Same as B, for lncRNAs. We analyzed 2,893 orthologous mouse and rat lncRNAs.

Figure 8. Conservation of developmental expression patterns of differentially expressed lncRNAs.

A. Comparison of the developmental stage in which maximum expression is observed, for orthologous lncRNAs that are significantly differentially expressed (FDR<0.01) among developmental stages, for both mouse and rat. The sample in which maximum expression is observed is computed based on average expression values across biological replicates, for each organ / developmental stage combination (Supplementary Methods). Genes are divided into classes based on the developmental stage where maximum expression is observed in mouse organs (X-axis). The Y axis represents the percentage of orthologous genes that reach maximum expression in each developmental stage, in the rat. Numbers of analyzed genes are shown below the plot.

B. Expression profiles of orthologous lncRNAs that are significantly differentially expressed (FDR<0.01) among developmental stages, for both mouse and rat, in the brain. TPM values were averaged across replicates and normalized by dividing by the maximum, for each species. The resulting relative expression profiles were combined across species and clustered with the K-means algorithm. Dots represent the average profiles of the genes belonging to each cluster. Gray lines represent profiles of individual genes from a cluster. Numbers of genes in each cluster are shown in the plot.

C. Same as B, for the kidney.

D. Same as B, for the liver.

E. Same as B, for the testes. For this organ, we searched for only 4 clusters with the K-means algorithm.

Figure 9. *Per*-gene estimates of expression pattern divergence between species.

A. Relationship between the per-gene expression divergence measure (Euclidean distance of relative expression profiles among organs/stages, between mouse and rat), and the average expression values (log2-transformed TPM) across all mouse and rat samples. We show a smoothed color density representation of the scatterplots, obtained through a 2D kernel density estimate (smoothScatter function in R). Red line: linear regression.

B. Distribution of the expression divergence value for all protein-coding and lncRNA genes with predicted 1-to-1 orthologues in mouse and rat.

C. Distribution of the residual expression divergence values, after regressing the average expression level, for protein-coding genes and lncRNAs.

D. Relationship between expression divergence and exonic sequence conservation (% exonic sequence aligned without gaps between mouse and rat), for protein-coding genes and lncRNAs.

E. Average contribution of each organ/developmental stage combination to expression divergence, for protein-coding genes and lncRNAs.

References

Altschul SF, Gish W, Miller W, Myers EW, Lipman DJ. 1990. Basic local alignment search tool. *J Mol Biol* 215: 403–410.

Amândio AR, Necsulea A, Joye E, Mascrez B, Duboule D. 2016. Hotair is dispensible for mouse development. *PLoS Genet* 12: e1006232.

Anders S, Huber W. 2010. Differential expression analysis for sequence count data. *Genome Biol* 11: R106.

Anderson KM, Anderson DM, McAnally JR, Shelton JM, Bassel-Duby R, Olson EN. 2016. Transcription of the non-coding RNA upperhand controls Hand2 expression and heart development. *Nature* 539: 433–436.

Ayers KL, Davidson NM, Demiyah D, Roeszler KN, Grützner F, Sinclair AH, Oshlack A, Smith CA. 2013. RNA sequencing reveals sexually dimorphic gene expression before gonadal differentiation in chicken and allows comprehensive annotation of the W-chromosome. *Genome Biol* 14.

Barutcu AR, Maass PG, Lewandowski JP, Weiner CL, Rinn JL. 2018. A TAD boundary is preserved upon deletion of the CTCF-rich Firre locus. *Nat Commun* 9: 1444.

Bassett AR, Akhtar A, Barlow DP, Bird AP, Brockdorff N, Duboule D, Ephrussi A, Ferguson-Smith AC, Gingeras TR, Haerty W, et al. 2014. Considerations when investigating lncRNA function in vivo. *eLife* 3: e03058.

Ben-Tabou de-Leon S, Davidson EH. 2007. Gene regulation: gene control network in development. *Annu Rev Biophys Biomol Struct* 36: 191.

Blanchette M, Kent WJ, Riemer C, Elnitski L, Smit AFA, Roskin KM, Baertsch R, Rosenbloom K, Clawson H, Green ED, et al. 2004. Aligning multiple genomic sequences with the threaded blockset aligner. *Genome Res* 14: 708–715.

Brannan CI, Dees EC, Ingram RS, Tilghman SM. 1990. The product of the H19 gene may function as an RNA. *Mol Cell Biol* 10: 28–36.

Brawand D, Soumillon M, Necsulea A, Julien P, Csárdi G, Harrigan P, Weier M, Liechti A, Aximu-Petri A, Kircher M, et al. 2011. The evolution of gene expression levels in mammalian organs. *Nature* 478: 343–348.

Bray NL, Pimentel H, Melsted P, Pachter L. 2016. Near-optimal probabilistic RNA-seq quantification. *Nat Biotechnol* 34: 525–527.

Brown CJ, Ballabio A, Rupert JL, Lafreniere RG, Grompe M, Tonlorenzi R, Willard HF. 1991. A gene from the region of the human X inactivation centre is expressed exclusively from the inactive X chromosome. *Nature* 349: 38–44.

Camacho C, Coulouris G, Avagyan V, Ma N, Papadopoulos J, Bealer K, Madden TL. 2009. BLAST+: architecture and applications. *BMC Bioinformatics* 10: 421.

Cardoso-Moreira M, Halbert J, Valloton D, Velten B, Chen C, Shao Y, Liechti A, Ascenção K, Rummel C, Ovchinnikova S, et al. 2019. Gene expression across mammalian organ development. *Nature* 571: 505–509.

Carelli FN, Hayakawa T, Go Y, Imai H, Warnefors M, Kaessmann H. 2016. The life history of retrocopies illuminates the evolution of new mammalian genes. *Genome Res* 26: 301–314.

Casper J, Zweig AS, Villarreal C, Tyner C, Speir ML, Rosenbloom KR, Raney BJ, Lee CM, Lee BT, Karolchik D, et al. 2018. The UCSC Genome Browser database: 2018 update. *Nucleic Acids Res* 46: D762–D769.

Cesana M, Cacchiarelli D, Legnini I, Santini T, Sthandier O, Chinappi M, Tramontano A, Bozzoni I. 2011. A long noncoding RNA controls muscle differentiation by functioning as a competing endogenous RNA. *Cell* 147: 358–369.

Cortez D, Marin R, Toledo-Flores D, Froidevaux L, Liechti A, Waters PD, Grützner F, Kaessmann H. 2014. Origins and functional evolution of Y chromosomes across mammals. *Nature* 508: 488–93.

Cunningham F, Achuthan P, Akanni W, Allen J, Amode MR, Armean IM, Bennett R, Bhai J, Billis K, Boddu S, et al. 2019. Ensembl 2019. *Nucleic Acids Res* 47: D745–D751.

Doolittle WF. 2018. We simply cannot go on being so vague about "function." *Genome Biol* 19: 223.

El-Gebali S, Mistry J, Bateman A, Eddy SR, Luciani A, Potter SC, Qureshi M, Richardson LJ, Salazar GA, Smart A, et al. 2019. The Pfam protein families database in 2019. *Nucleic Acids Res* 47: D427–D432.

Engreitz JM, Haines JE, Perez EM, Munson G, Chen J, Kane M, McDonel PE, Guttman M, Lander ES. 2016. Local regulation of gene expression by lncRNA promoters, transcription and splicing. *Nature* 539: 452–455.

Goudarzi M, Berg K, Pieper LM, Schier AF. 2019. Individual long non-coding RNAs have no overt functions in zebrafish embryogenesis, viability and fertility. *eLife* 8.

Graur D, Zheng Y, Price N, Azevedo RBR, Zufall RA, Elhaik E. 2013. On the immortality of television sets: "function" in the human genome according to the evolution-free gospel of ENCODE. *Genome Biol Evol* 5: 578–590.

Green CD, Ma Q, Manske GL, Shami AN, Zheng X, Marini S, Moritz L, Sultan C, Gurczynski SJ, Moore BB, et al. 2018. A comprehensive roadmap of murine spermatogenesis defined by single-cell RNA-Seq. *Dev Cell* 46: 651-667.e10.

Groff AF, Sanchez-Gomez DB, Soruco MML, Gerhardinger C, Barutcu AR, Li E, Elcavage L, Plana O, Sanchez LV, Lee JC, et al. 2016. In vivo characterization of Linc-p21 reveals functional cis-regulatory DNA elements. *Cell Rep* 16: 2178–2186.

Grote P, Herrmann BG. 2015. Long noncoding RNAs in organogenesis: making the difference. *Trends Genet TIG* 31: 329–335.

Grote P, Wittler L, Hendrix D, Koch F, Währisch S, Beisaw A, Macura K, Bläss G, Kellis M, Werber M, et al. 2013. The tissue-specific lncRNA Fendrr is an essential regulator of heart and body wall development in the mouse. *Dev Cell* 24: 206–214.

Guttman M, Amit I, Garber M, French C, Lin MF, Feldser D, Huarte M, Zuk O, Carey BW, Cassady JP, et al. 2009. Chromatin signature reveals over a thousand highly conserved large non-coding RNAs in mammals. *Nature* 458: 223–227.

1014 Hacisuleyman E, Goff LA, Trapnell C, Williams A, Henao-Mejia J, Sun L, McClanahan P, Hendrickson DG,
1015 Sauvageau M, Kelley DR, et al. 2014. Topological organization of multichromosomal regions by
1016 the long intergenic noncoding RNA Firre. *Nat Struct Mol Biol* 21: 198–206.

1017 Haerty W, Ponting CP. 2013. Mutations within lncRNAs are effectively selected against in fruitfly but
1018 not in human. *Genome Biol* 14: R49.

1019 Haerty W, Ponting CP. 2014. No gene in the genome makes sense except in the light of evolution. *Annu*
1020 *Rev Genomics Hum Genet* 15: 71–92.

1021 Haerty W, Ponting CP. 2015. Unexpected selection to retain high GC content and splicing enhancers
1022 within exons of multiexonic lncRNA loci. *RNA N Y N* 21: 333–346.

1023 Hamburger V, Hamilton HL. 1951. A series of normal stages in the development of the chick embryo. *J*
1024 *Morphol* 88: 49–92.

1025 Hezroni H, Koppstein D, Schwartz MG, Avrutin A, Bartel DP, Ulitsky I. 2015. Principles of long noncoding
1026 RNA evolution derived from direct comparison of transcriptomes in 17 species. *Cell Rep* 11:
1027 1110–1122.

1028 Iyer MK, Niknafs YS, Malik R, Singhal U, Sahu A, Hosono Y, Barrette TR, Prensner JR, Evans JR, Zhao S,
1029 et al. 2015. The landscape of long noncoding RNAs in the human transcriptome. *Nat Genet* 47:
1030 199–208.

1031 Kaessmann H. 2010. Origins, evolution, and phenotypic impact of new genes. *Genome Res* 20: 1313–
1032 1326.

1033 Kapusta A, Kronenberg Z, Lynch VJ, Zhuo X, Ramsay L, Bourque G, Yandell M, Feschotte C. 2013.
1034 Transposable elements are major contributors to the origin, diversification, and regulation of
1035 vertebrate long noncoding RNAs. *PLoS Genet* 9: e1003470.

1036 Khalil AM, Guttman M, Huarte M, Garber M, Raj A, Rivea Morales D, Thomas K, Presser A, Bernstein
1037 BE, van Oudenaarden A, et al. 2009. Many human large intergenic noncoding RNAs associate
1038 with chromatin-modifying complexes and affect gene expression. *Proc Natl Acad Sci U S A* 106:
1039 11667–11672.

1040 Kim D, Langmead B, Salzberg SL. 2015. HISAT: a fast spliced aligner with low memory requirements.
1041 *Nat Methods* 12: 357–60.

1042 Kutter C, Watt S, Stefflova K, Wilson MD, Goncalves A, Ponting CP, Odom DT, Marques AC. 2012. Rapid
1043 turnover of long noncoding RNAs and the evolution of gene expression. *PLoS Genet* 8:
1044 e1002841.

1045 Latos PA, Pauler FM, Koerner MV, Şenergin HB, Hudson QJ, Stocsits RR, Allhoff W, Stricker SH, Klement
1046 RM, Warczok KE, et al. 2012. Airn transcriptional overlap, but not its lncRNA products, induces
1047 imprinted Igf2r silencing. *Science* 338: 1469–1472.

1048 Liao Y, Smyth GK, Shi W. 2019. The R package Rsubread is easier, faster, cheaper and better for
1049 alignment and quantification of RNA sequencing reads. *Nucleic Acids Res*.

1050 Lin MF, Carlson JW, Crosby MA, Matthews BB, Yu C, Park S, Wan KH, Schroeder AJ, Gramates LS, St
1051 Pierre SE, et al. 2007. Revisiting the protein-coding gene catalog of Drosophila melanogaster
1052 using 12 fly genomes. *Genome Res* 17: 1823–1836.

Lin MF, Jungreis I, Kellis M. 2011. PhyloCSF: a comparative genomics method to distinguish protein coding and non-coding regions. *Bioinforma Oxf Engl* 27: i275-282.

Liu SJ, Nowakowski TJ, Pollen AA, Lui JH, Horlbeck MA, Attenello FJ, He D, Weissman JS, Kriegstein AR, Diaz AA, et al. 2016. Single-cell analysis of long non-coding RNAs in the developing human neocortex. *Genome Biol* 17: 67.

Love MI, Huber W, Anders S. 2014. Moderated estimation of fold change and dispersion for RNA-seq data with DESeq2. *Genome Biol* 15: 550.

Marques AC, Hughes J, Graham B, Kowalczyk MS, Higgs DR, Ponting CP. 2013. Chromatin signatures at transcriptional start sites separate two equally populated yet distinct classes of intergenic long noncoding RNAs. *Genome Biol* 14: R131.

McCarthy FM, Pendarvis K, Cooksey AM, Gresham CR, Bomhoff M, Davey S, Lyons E, Sonstegard TS, Bridges SM, Burgess SC. 2019. Chickspress: a resource for chicken gene expression. *Database* 2019. https://academic.oup.com/database/article/doi/10.1093/database/baz058/5512474 (Accessed August 11, 2019).

McDonald JH, Kreitman M. 1991. Adaptive protein evolution at the Adh locus in Drosophila. *Nature* 351: 652–654.

Munschauer M, Nguyen CT, Sirokman K, Hartigan CR, Hogstrom L, Engreitz JM, Ulirsch JC, Fulco CP, Subramanian V, Chen J, et al. 2018. The NORAD lncRNA assembles a topoisomerase complex critical for genome stability. *Nature* 561: 132–136.

Necsulea A, Soumillon M, Warnefors M, Liechti A, Daish T, Grutzner F, Kaessmann H. 2014. The evolution of lncRNA repertoires and expression patterns in tetrapods. *Nature* 505: 635–640.

Nel-Themaat L, Gonzalez G, Akiyama H, Behringer RR. 2010. Illuminating testis morphogenesis in the mouse. *J Androl* 31: 5–10.

Ørom UA, Derrien T, Beringer M, Gumireddy K, Gardini A, Bussotti G, Lai F, Zytnicki M, Notredame C, Huang Q, et al. 2010. Long noncoding RNAs with enhancer-like function in human cells. *Cell* 143: 46–58.

Pertea M, Pertea GM, Antonescu CM, Chang T-C, Mendell JT, Salzberg SL. 2015. StringTie enables improved reconstruction of a transcriptome from RNA-seq reads. *Nat Biotechnol* 33: 290–5.

Pertea M, Shumate A, Pertea G, Varabyou A, Breitwieser FP, Chang Y-C, Madugundu AK, Pandey A, Salzberg SL. 2018. CHESS: a new human gene catalog curated from thousands of large-scale RNA sequencing experiments reveals extensive transcriptional noise. *Genome Biol* 19: 208.

Ponjavic J, Ponting CP, Lunter G. 2007. Functionality or transcriptional noise? Evidence for selection within long noncoding RNAs. *Genome Res* 17: 556–65.

R Core Team. 2018. *R: A Language and Environment for Statistical Computing*. https://www.R-project.org/.

Rinn JL, Kertesz M, Wang JK, Squazzo SL, Xu X, Brugmann SA, Goodnough LH, Helms JA, Farnham PJ, Segal E, et al. 2007. Functional demarcation of active and silent chromatin domains in human HOX loci by noncoding RNAs. *Cell* 129: 1311–1323.

1091 Sarropoulos I, Marin R, Cardoso-Moreira M, Kaessmann H. 2019. Developmental dynamics of lncRNAs
1092 across mammalian organs and species. *Nature* 571: 510–514.

1093 Sauvageau M, Goff LA, Lodato S, Bonev B, Groff AF, Gerhardinger C, Sanchez-Gomez DB, Hacisuleyman
1094 E, Li E, Spence M, et al. 2013. Multiple knockout mouse models reveal lincRNAs are required
1095 for life and brain development. *eLife* 2: e01749.

1096 Schüler A, Ghanbarian AT, Hurst LD. 2014. Purifying selection on splice-related motifs, not expression
1097 level nor RNA folding, explains nearly all constraint on human lincRNAs. *Mol Biol Evol* 31: 3164–
1098 3183.

1099 Siepel A, Bejerano G, Pedersen JS, Hinrichs AS, Hou M, Rosenbloom K, Clawson H, Spieth J, Hillier LW,
1100 Richards S, et al. 2005. Evolutionarily conserved elements in vertebrate, insect, worm, and
1101 yeast genomes. *Genome Res* 15: 1034–50.

1102 Smedley D, Haider S, Ballester B, Holland R, London D, Thorisson G, Kasprzyk A. 2009. BioMart--
1103 biological queries made easy. *BMC Genomics* 10: 22.

1104 Smit AFA, Hubley R, Green P. 2003. *RepeatMasker Open-4.0.* http://www.repeatmasker.org.

1105 Soumillon M, Necsulea A, Weier M, Brawand D, Zhang X, Gu H, Barthès P, Kokkinaki M, Nef S, Gnirke
1106 A, et al. 2013. Cellular source and mechanisms of high transcriptome complexity in the
1107 mammalian testis. *Cell Rep* 3: 2179–2190.

1108 Tabula Muris Consortium. 2018. Single-cell transcriptomics of 20 mouse organs creates a Tabula Muris.
1109 *Nature* 562: 367–372.

1110 Theiler K. 1989. *The house mouse: atlas of embryonic development*. Springer-Verlag, Berlin Heidelberg
1111 https://www.springer.com/la/book/9783642884207.

1112 The UniProt Consortium. 2017. UniProt: the universal protein knowledgebase. *Nucleic Acids Res* 45:
1113 D158–D169.

1114 Uebbing S, Konzer A, Xu L, Backström N, Brunström B, Bergquist J, Ellegren H. 2015. Quantitative mass
1115 spectrometry reveals partial translational regulation for dosage compensation in chicken. *Mol*
1116 *Biol Evol* 32: 2716–2725.

1117 Ulitsky I. 2016. Evolution to the rescue: using comparative genomics to understand long non-coding
1118 RNAs. *Nat Rev Genet* 17: 601–614.

1119 Ulitsky I, Shkumatava A, Jan CH, Sive H, Bartel DP. 2011. Conserved function of lincRNAs in vertebrate
1120 embryonic development despite rapid sequence evolution. *Cell* 147: 1537–1550.

1121 Vendramin R, Verheyden Y, Ishikawa H, Goedert L, Nicolas E, Saraf K, Armaos A, Delli Ponti R,
1122 Izumikawa K, Mestdagh P, et al. 2018. SAMMSON fosters cancer cell fitness by concertedly
1123 enhancing mitochondrial and cytosolic translation. *Nat Struct Mol Biol* 25: 1035–1046.

1124 Villar D, Berthelot C, Aldridge S, Rayner TF, Lukk M, Pignatelli M, Park TJ, Deaville R, Erichsen JT,
1125 Jasinska AJ, et al. 2015. Enhancer evolution across 20 mammalian species. *Cell* 160: 554–566.

1126 Washietl S, Kellis M, Garber M. 2014. Evolutionary dynamics and tissue specificity of human long
1127 noncoding RNAs in six mammals. *Genome Res* 24: 616–28.

1128 Zakany J, Darbellay F, Mascrez B, Necsulea A, Duboule D. 2017. Control of growth and gut maturation
1129 by HoxD genes and the associated lncRNA Haglr. *Proc Natl Acad Sci U S A* 114: E9290–E9299.

1130

Darbellay and Necsulea, Figure 1

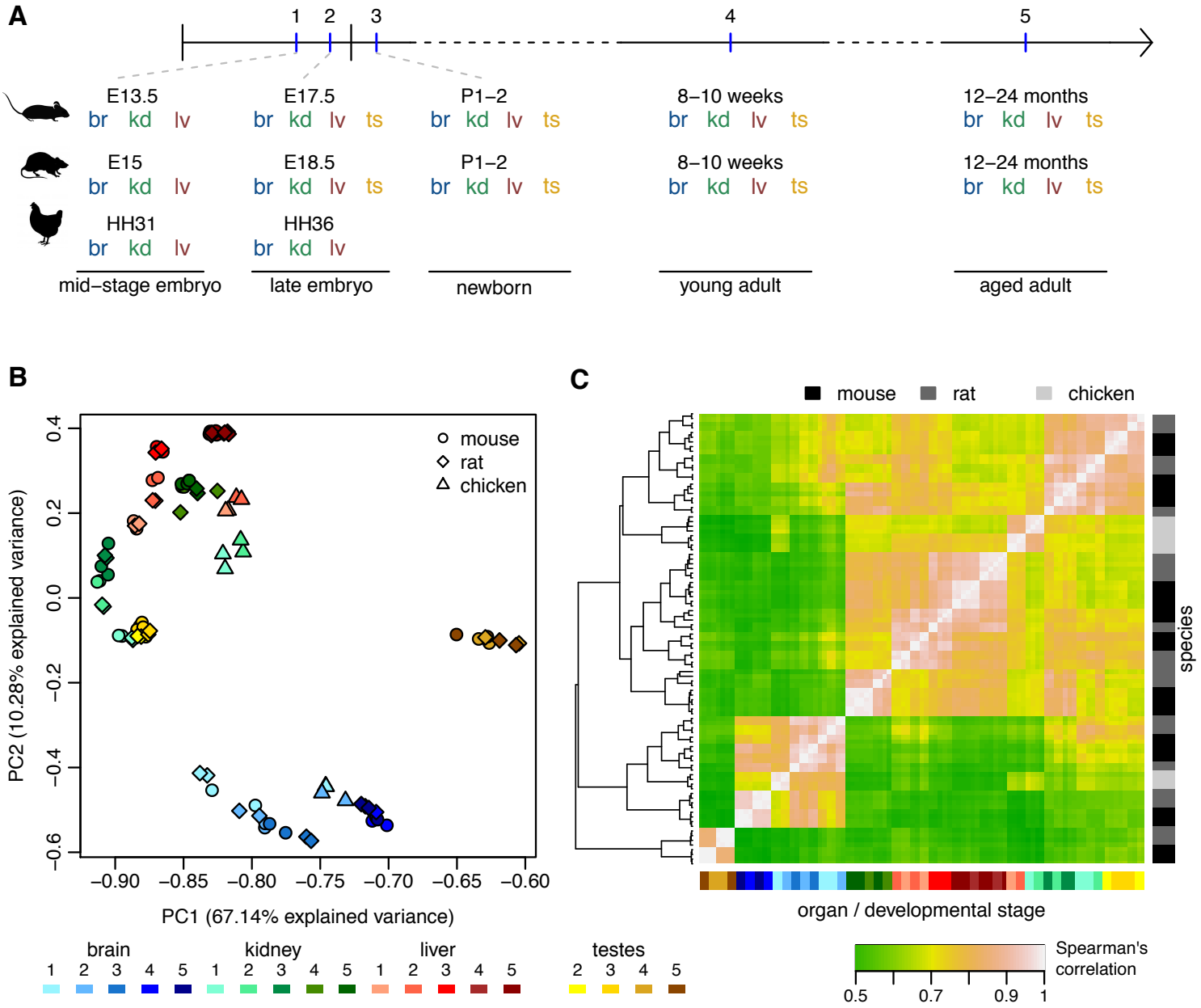

Darbellay and Necsulea, Figure 2

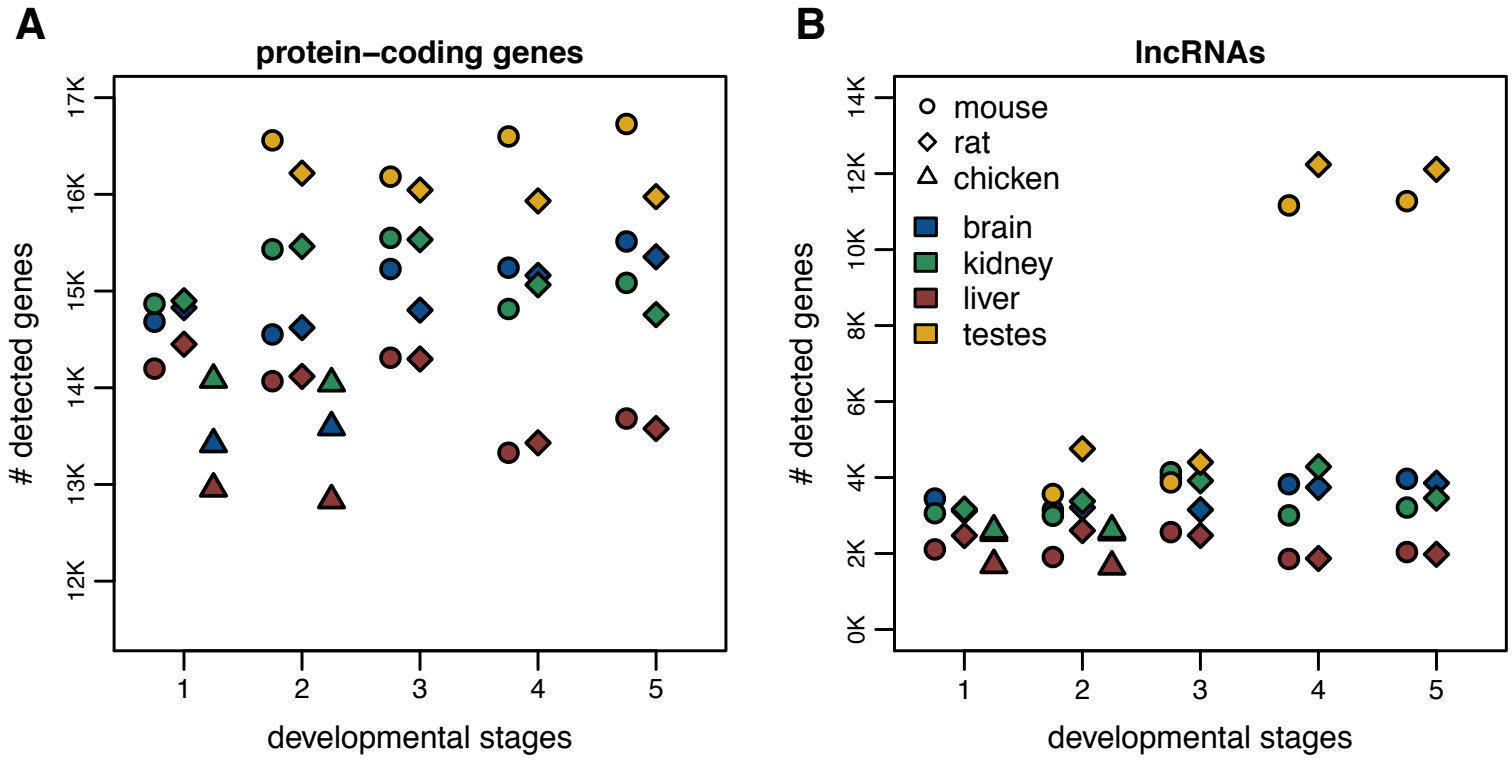

Darbellay and Necsulea, Figure 3

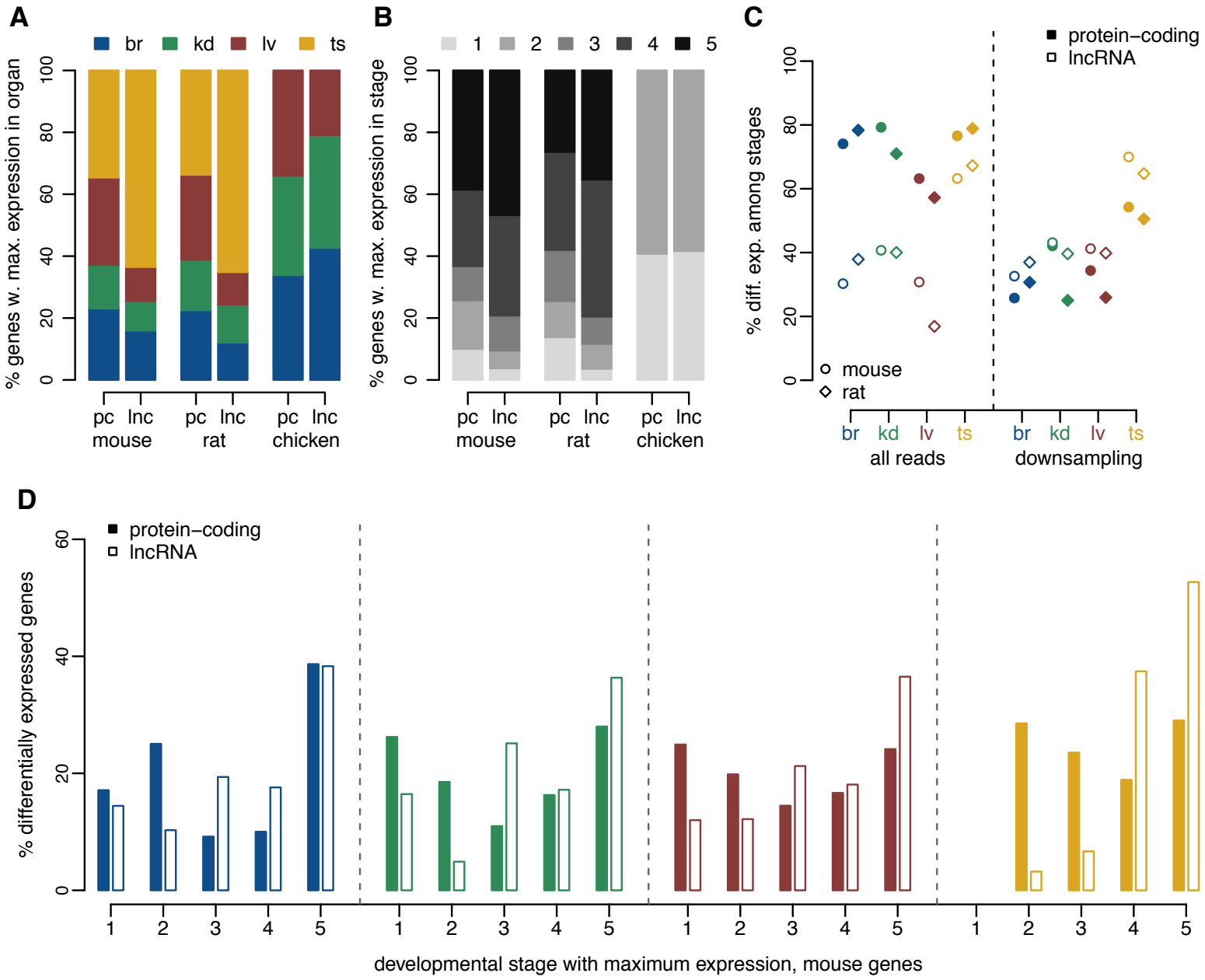

Darbellay and Necsulea, Figure 4

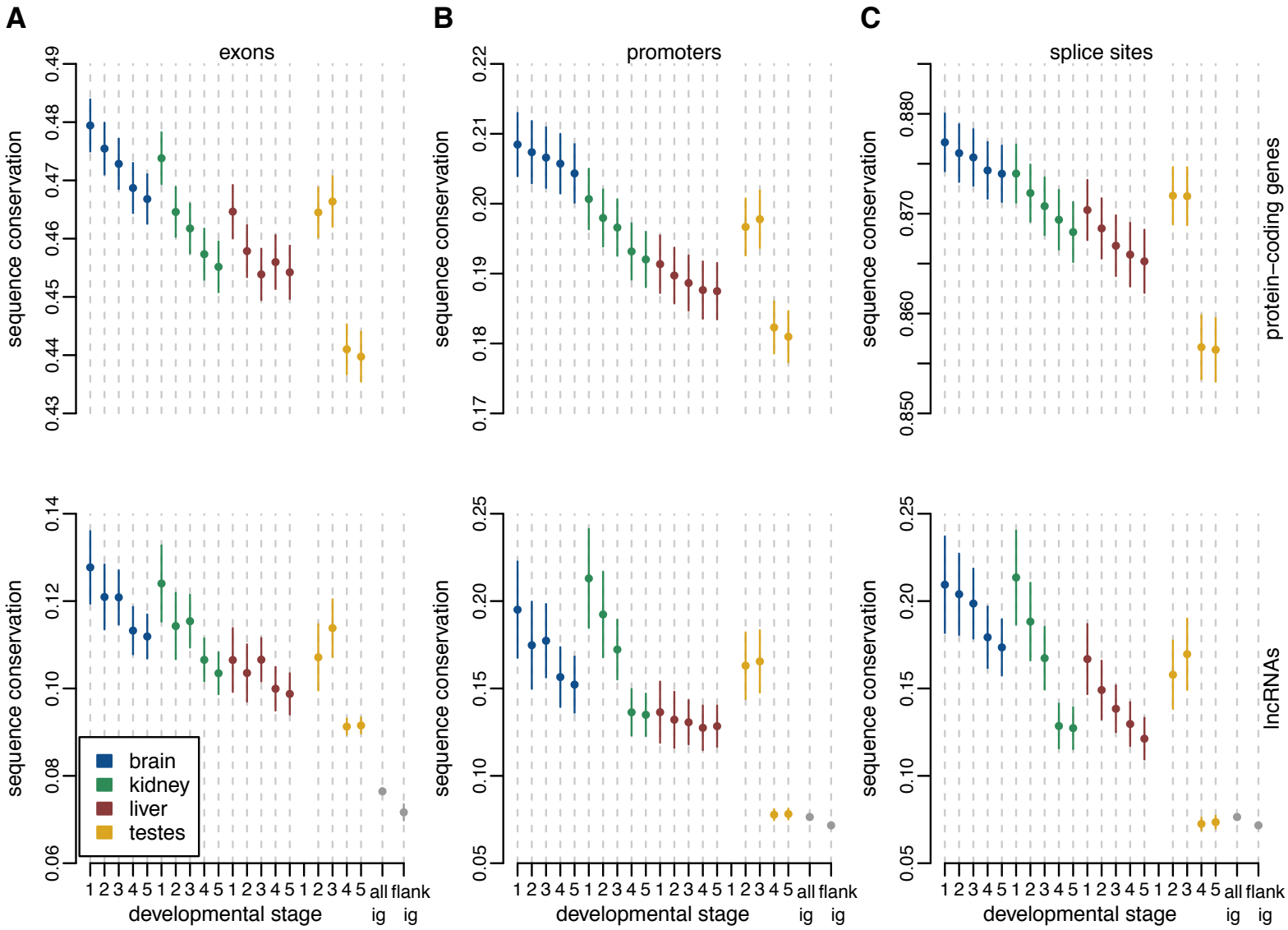

Darbellay and Necsulea, Figure 5

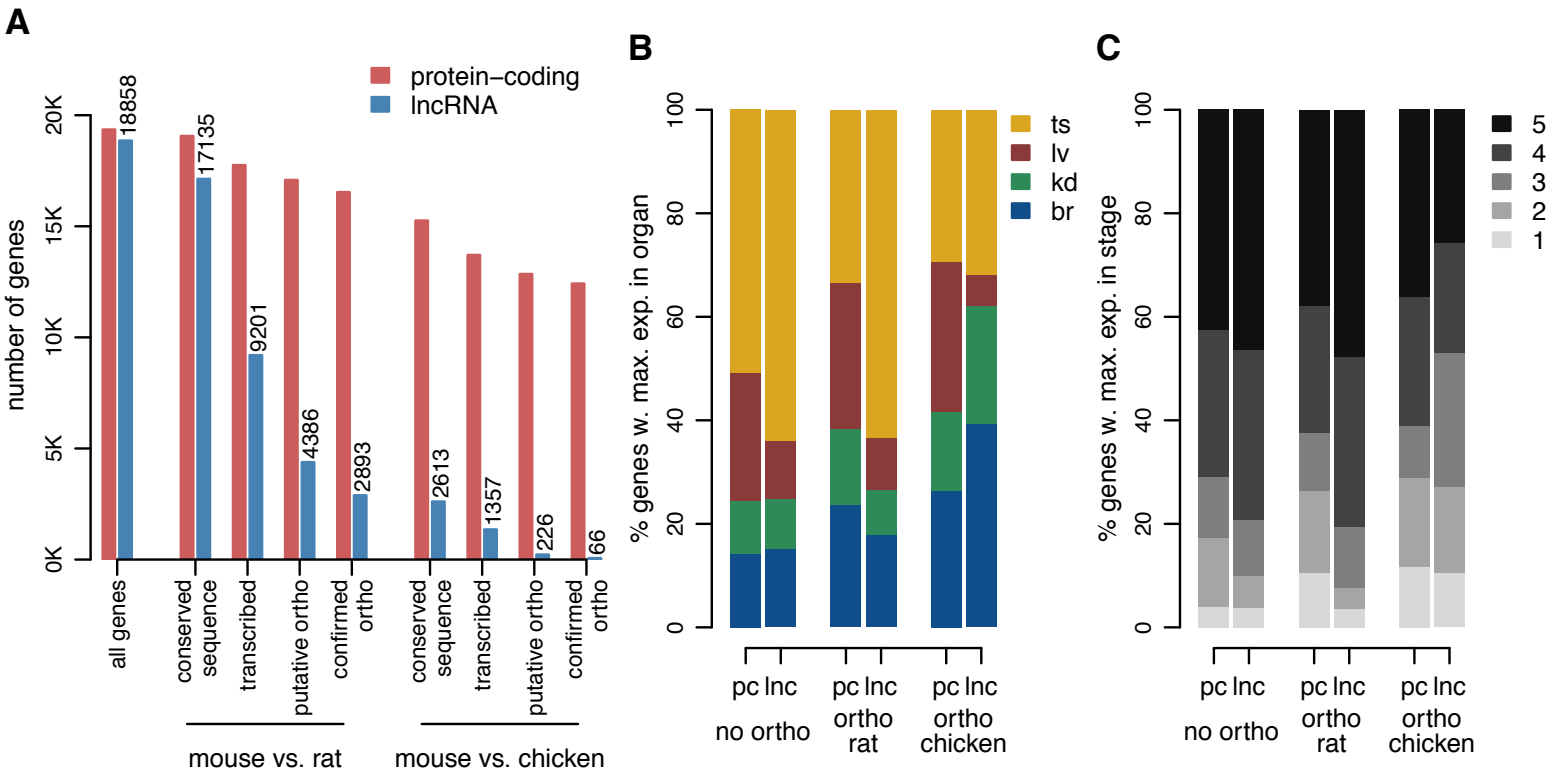

Darbellay and Necsulea, Figure 6

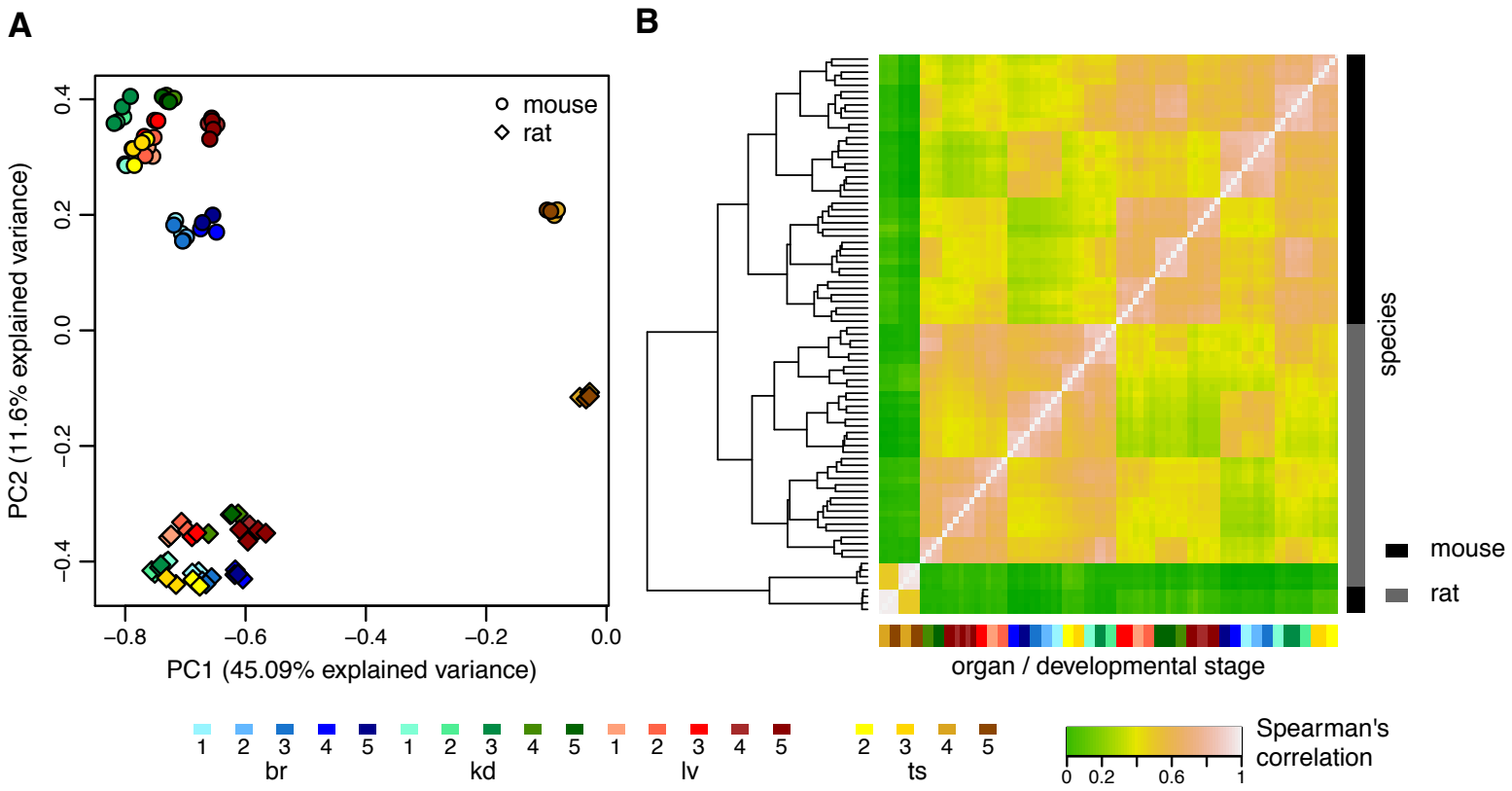

Darbellay and Necsulea, Figure 7

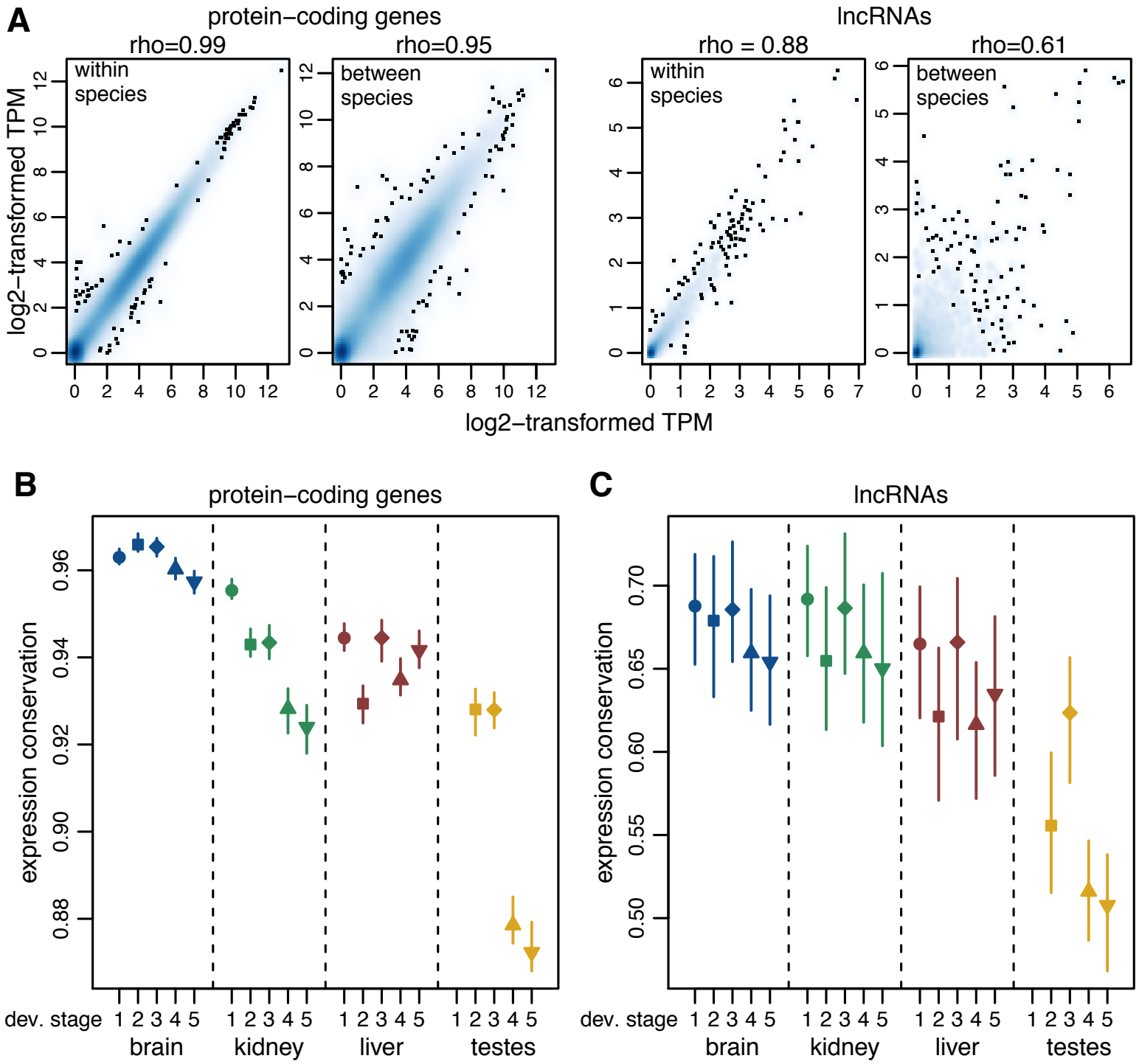

Darbellay and Necsulea, Figure 8

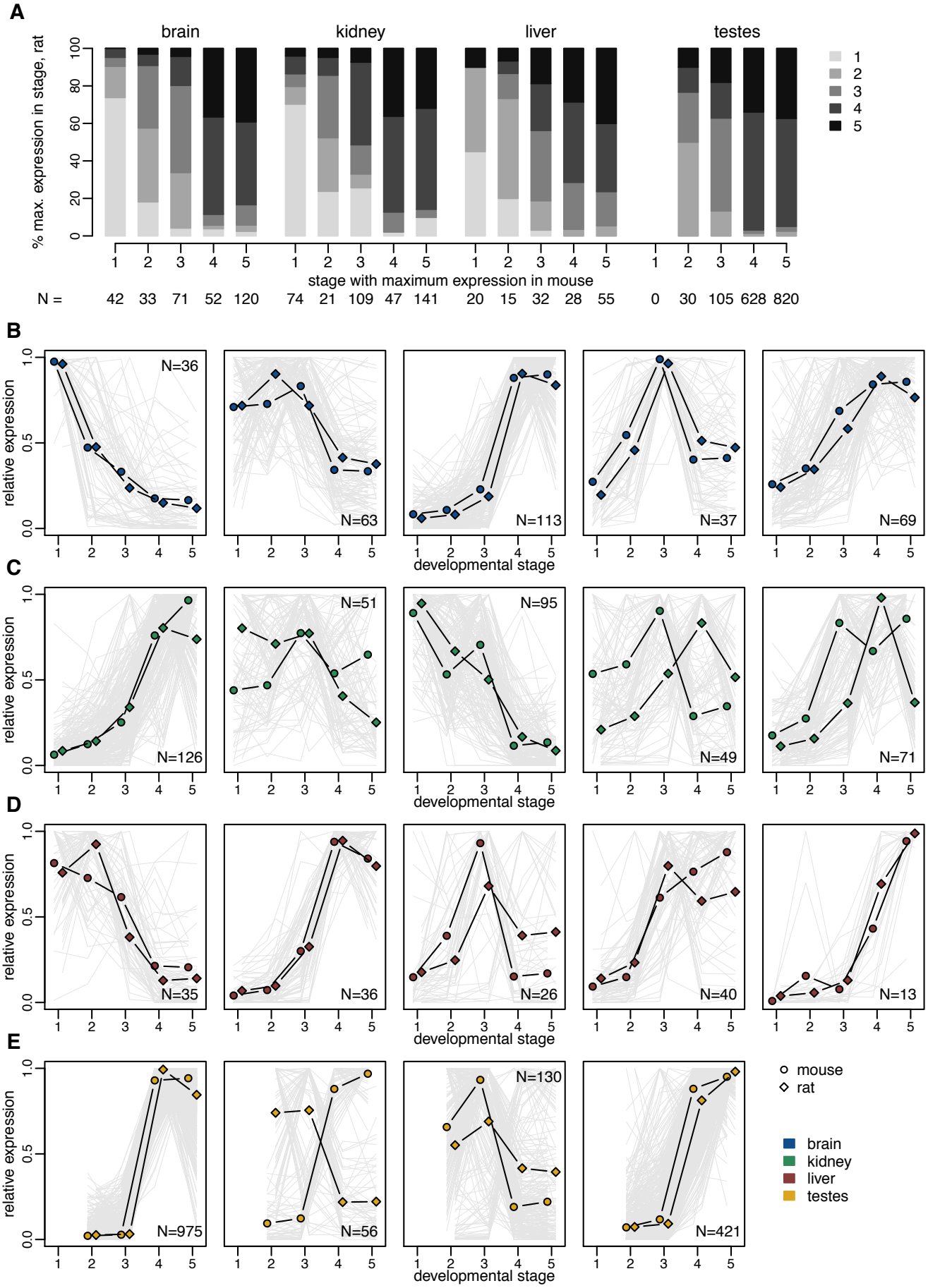

Darbellay and Necsulea, Figure 9